Mainshocks are aftershocks of conditional foreshocks: how to foreshock statistical properties emerge from aftersock laws.

Agnès Helmstetter, D. Sornette, Jean-Robert Grasso

Mainshocks are Aftershocks of Conditional Foreshocks: How do Foreshock Statistical Properties Emerge from Aftershock Laws

Agnès Helmstetter
Laboratoire de Géophysique Interne et Tectonophysique, Observatoire de Grenoble, Université Joseph Fourier, France

Didier Sornette
Laboratoire de Physique de la Matière Condensée, CNRS UMR 6622 Université de Nice-Sophia Antipolis, Parc Valrose, 06108 Nice, France and Department of Earth and Space Sciences and Institute of Geophysics and Planetary Physics, University of California, Los Angeles, California 90095-1567

Jean-Robert Grasso
Laboratoire de Géophysique Interne et Tectonophysique, Observatoire de Grenoble, Université Joseph Fourier, France

Abstract

The inverse Omori law for foreshocks discovered in the 1970s states that the rate of earthquakes prior to a mainshock increases on average as a power law $\propto 1/(t_c - t)^{p'}$ of the time to the mainshock occurring at t_c. Here, we show that this law results from the direct Omori law for aftershocks describing the power law decay $\sim 1/(t - t_c)^p$ of seismicity after an earthquake, provided that any earthquake can trigger its suit of aftershocks. In this picture, the seismic activity at any time is the sum of the spontaneous tectonic loading and of the activity triggered by all preceding events weighted by their corresponding Omori law. The inverse Omori law then emerges as the expected (in a statistical sense) trajectory of seismicity, conditioned on the fact that it leads to the burst of seismic activity accompanying the mainshock. In particular, we predict and verify by numerical simulations on the Epidemic-Type-Aftershock Sequence (ETAS) model that p' is always smaller than or equal to p and a function of p, of the b-value of the Gutenberg-Richter law (GR) and of a parameter quantifying the number of direct aftershocks as a function of the magnitude of the mainshock. The often documented apparent decrease of the b-value of the GR law at the approach to the main shock results straightforwardly from the conditioning of the path of seismic activity culminating at the mainshock. However, we predict that the GR law is not modified simply by a change of b-value but that a more accurate statement is that the GR law gets an additive (or deviatoric) power law contribution with exponent smaller than b and with an amplitude growing as a power law of the time to the mainshock. In the space domain, we predict that the phenomenon of aftershock diffusion must have its mirror process reflected into an inward migration of foreshocks towards the mainshock. In this model, foreshock sequences are special aftershock sequences which are modified by the condition to end up in a burst of seismicity associated with the mainshock. Foreshocks are not

just statistical creatures, they are genuine forerunners of large shocks as shown by the large prediction gains obtained using several of their qualifiers.

1. Introduction

Large shallow earthquakes are followed by an increase in seismic activity, defined as an aftershock sequence. It is also well-known that large earthquakes are sometimes preceded by an unusually large activity rate, defined as a foreshock sequence. Omori law describing the power law decay $\sim 1/(t-t_c)^p$ of aftershock rate with time from a mainshock that occurred at t_c has been proposed more than one century ago [*Omori*, 1894], and has since been verified by many studies [*Kagan and Knopoff*, 1978; *Davis and Frohlich*, 1991; *Kisslinger and Jones*, 1991; *Utsu et al.*, 1995]. See however [*Kisslinger*, 1993; *Gross and Kisslinger*, 1994] for alternative decay laws such as the stretched exponential and its possible explanation [*Helmstetter and Sornette*, 2002a].

Whereas the Omori law describing the aftershock decay rate is one of the few well-established empirical laws in seismology, the increase of foreshock rate before an earthquake does not follow such a well-defined empirical law. There are huge fluctuations of the foreshock seismicity rate, if any, from one sequence of earthquakes to another one preceding a mainshock. Moreover, the number of foreshocks per mainshock is usually quite smaller than the number of aftershocks. It is thus essentially impossible to establish a deterministic empirical law that describes the intermittent increase of seismic activity prior to a mainshock when looking at a single foreshock sequence which contains at best a few events. Although well-developed individual foreshock sequences are rare and mostly irregular, a well-defined acceleration of foreshock rate prior to a mainshock emerges when using a superposed epoch analysis, in other words, by synchronizing several foreshock sequences to a common origin of time defined as the time of their mainshocks and by stacking these synchronized foreshock sequences. In this case, the acceleration of the seismicity preceding the mainshock clearly follows an inverse Omori law of the form $N(t) \sim 1/(t_c-t)^{p'}$, where t_c is the time of the mainshock. This law has been first proposed by *Papazachos* [1973], and has been established more firmly by [*Kagan and Knopoff*, 1978; *Jones and Molnar*, 1979]. The inverse Omori law is usually observed for time scales smaller than the direct Omori law, of the order of weeks to months before the mainshock.

A clear identification of foreshocks, aftershocks and mainshocks is hindered by the difficulties in associating an unambiguous and unique space-time-magnitude domain to any earthquake sequence. Identifying aftershocks and foreshocks requires the definition of a space-time window. All events in the same space-time domain define a sequence. The largest earthquake in the sequence is called the mainshock. The following events are identified as aftershocks, and the preceding events are called foreshocks.

Large aftershocks show the existence of secondary aftershock activities, that is, the fact that aftershocks may have their own aftershocks, such as the $M = 6.5$ Big Bear event, which is considered as an aftershock of the $M = 7.2$ Landers Californian earthquake, and which clearly triggered its own aftershocks. Of course, the aftershocks of aftershocks can be clearly identified without further insight and analysis as obvious bursts of transient seismic activity above the background seismicity level, only for the largest aftershocks. But because aftershocks exist on all scales, from the laboratory scale, e.g. [*Mogi*, 1967; *Scholz*, 1968], to the worldwide seismicity, we may expect that all earthquakes, whatever their magnitude, trigger their own aftershocks, but with a rate increasing with the mainshock magnitude, so that only aftershocks of the largest earthquakes are identifiable unambiguously.

The properties of aftershock and foreshock sequences depend on the choice of these space-time windows, and on the specific definition of foreshocks [e.g. *Ogata et al.*, 1996], which can sometimes be rather arbitrary. In the sequel, we shall consider two definitions of foreshocks for a given space and time window:

1. we shall call "foreshock" of type I any event of magnitude smaller than or equal to the magnitude of the following event, then identified as a "main shock". This definition implies the choice of a space-time window $R \times TT$ used to define both foreshocks and mainshocks. Mainshocks are large earthquakes that were not preceded by a larger event in this space-time window. The same window is used to select foreshocks before mainshocks;

2. we shall also consider "foreshock" of type II, as any earthquake preceding a large earthquake, defined as the mainshock, independently of the relative magnitude of the foreshock compared to that of the mainshock. This second definition will thus incorporate seismic sequences in which a foreshock could have a magnitude larger than the mainshock, a situation which can alternatively be interpreted as a mainshock followed by a large aftershock.

The advantage of this second definition is that foreshocks of type II are automatically defined as soon as one has identified the mainshocks, for instance, by calling mainshocks all events of magnitudes larger than some threshold of interest. Foreshocks of type II are thus all events preceding these large magnitude mainshocks. In contrast, foreshocks of type I need to obey a constraint on their magnitude, which may be artificial, as suggested from the previous discussion. All studies published in the literature deal with foreshocks of type I. Using a very simple model of seismicity, the so-called ETAS (epidemic-type aftershock) model, we shall show that the definition of foreshocks of type II is also quite meaningful and provides new insights for classifying earthquake phenomenology and understanding earthquake clustering in time and space.

The exponent p' of the inverse Omori law is usually found to be smaller than or close to 1 [*Papazachos et al.*, 1967; *Papazachos et al.*, 1975b; *Kagan and Knopoff*, 1978; *Jones and Molnar*, 1979; *Davis and Frohlich*, 1991; *Shaw*, 1993; *Ogata et al.*, 1995; *Maeda*, 1999; *Reasenberg*, 1999], and is always found smaller than or equal to the direct Omori exponent p when the 2 exponents p and p' are measured simultaneously on the same mainshocks [*Kagan and Knopoff*, 1978; *Davis and Frohlich*, 1991; *Shaw*, 1993; *Maeda*, 1999; *Reasenberg*, 1999]. *Shaw* [1993] suggested in a peculiar case the relationship $p' = 2p - 1$, based on a clever but slightly incorrect reasoning (see below). We shall recover below this relationship only in a certain regime of the ETAS model from an exact treatment of the foreshocks of type II within the framework of the ETAS model.

Other studies tried to fit a power law increase of seismicity to individual foreshock sequences. Rather than the number of foreshocks, these studies usually fit the cumulative Benioff strain release ϵ by a power-law $\epsilon(t) = \epsilon_c - B(t_c - t)^z$ with an exponent z that is often found close to 0.3 (see [*Jaumé and Sykes*, 1999; *Sammis and Sornette*, 2002] for reviews). Assuming a constant Gutenberg Richter b-value through time, so that the acceleration of the cumulative Benioff strain before the mainshock is due only to the increase in the seismicity rate, this would argue for a p'-value close to 0.7. These studies were often motivated by the critical point theory [*Sornette and Sammis*, 1995], which predicts a power-law increase of seismic activity before major earthquakes (see e.g. [*Sammis and Sornette*, 2002] for a review). However, the statistical significance of such a power-acceleration of energy before individual mainshock is still controversial [*Zöller and Hainzl*, 2002].

The frequency-size distribution of foreshocks has also been observed either to be different from that of aftershocks, $b' < b$, e.g. [*Suyehiro*, 1966; *Papazachos et al.*, 1967; *Ikegami*, 1967; *Berg*, 1968], or to change as the mainshock is approached. This change of magnitude distribution is often interpreted as a decrease of b-value, first reported by [*Kagan and Knopoff*, 1978; *Li et al.*, 1978; *Wu et al.*, 1978]. Others studies suggest that the modification of the magnitude distribution is due only to moderate or large events, whereas the distribution of small magnitude events is not modified [*Rotwain et al.*, 1997; *Jaumé and Sykes*, 1999]. *Knopoff et al.* [1982] state that only in the rare cases of catalogs of great length, statistically significant smaller b-value for foreshocks than for aftershocks are found. Nevertheless they believe the effect is likely to be real in most catalogs, but at a very low level of difference.

On the theoretical front, there have been several models developed to account for foreshocks. Because foreshocks are rare and seem the forerunners of large events, a natural approach is to search for physical mechanisms that may explain their specificity. And, if there is a specificity, this might lead to the use of foreshocks as precursory patterns for earthquake prediction. Foreshocks may result from a slow subcritical weakening by stress corrosion [*Yamashita and Knopoff*, 1989, 1992; *Shaw*, 1993] or from a general damage process [*Sornette et al.*, 1992]. The same mechanism can also reproduce aftershock behavior [*Yamashita and Knopoff*, 1987; *Shaw*, 1993]. Foreshocks and aftershocks may result also from the dynamics of stress distribution on pre-existing hierarchical structures of faults or tectonic blocks [*Huang et al.*, 1998; *Gabrielov et al.*, 2000a,b; *Narteau et al.*, 2000], when assuming that the scale over which stress redistribution occurs is controlled by the level of the hierarchy (cell size in a hierarchical cellular automaton model). *Dodge et al.* [1996] argue that foreshocks are a byproduct of an aseismic nucleation process of a mainshock. Other possible mechanisms for both aftershocks and foreshocks are based on the visco-elastic response of the crust and on delayed transfer of fluids in and out of fault structures [*Hainzl et al.*, 1999; *Pelletier*, 2000].

Therefore, most of these models suggest a link between aftershocks and foreshocks. In the present work, we explore this question further by asking the following question: is it possible to derive most if

not all of the observed phenomenology of foreshocks from the knowledge of only the most basic and robust facts of earthquake phenomenology, namely the Gutenberg-Richter and Omori laws? To address this question, we use what is maybe the simplest statistical model of seismicity, the so-called ETAS (epidemic-type aftershock) model, based only on the Gutenberg-Richter and Omori laws. This model assumes that each earthquake can trigger aftershocks, with a rate increasing as a power law E^a with the mainshock energy E, and which decays with the time from the mainshock according to the "local" Omori law $\sim 1/(t-t_c)^{1+\theta}$, with $\theta \geq 0$. We stress that the exponent $1+\theta$ is in general different from the observable p-value, as we shall explain below. In this model, the seismicity rate is the result of the whole cascade of direct and secondary aftershocks, that is, aftershocks of aftershocks, aftershocks of aftershocks of aftershocks, and so on.

In two previous studies of this model, we have analyzed the super-critical regime [*Helmstetter and Sornette*, 2002a] and the singular regime [*Sornette and Helmstetter*, 2002] of the ETAS model and have shown that these regimes can produce respectively an exponential or a power law acceleration of the seismicity rate. These results can reproduce an individual accelerating foreshock sequence, but they cannot model the stationary seismicity with alternative increasing and decreasing seismicity rate before and after a large earthquake. In this study, we analyze the stationary sub-critical regime of this branching model and we show that foreshock sequences are special aftershock sequences which are modified by the condition to end up in a burst of seismicity associated with the mainshock. Using only the physics of aftershocks, all the foreshock phenomenology is derived analytically and verified accurately by our numerical simulations. This is related to but fundamentally different from the proposal by *Jones et al.* [1999] that foreshocks are mainshocks whose aftershocks happen to be big.

Our analytical and numerical investigation of the ETAS model gives the main following results:

- In the ETAS model, the rate of foreshocks increases before the mainshock according to the inverse Omori law $N(t) \sim 1/(t_c-t)^{p'}$ with an exponent p' smaller than the exponent p of the direct Omori law. The exponent p' depends on the local Omori exponent $1+\theta$, on the exponent β of the energy distribution, and on the exponent a which describes the increase in the number of aftershocks with the mainshock energy. In contrast with the direct Omori law, which is clearly observed after all large earthquakes, the inverse Omori law is a statistical law, which is observed only when stacking many foreshock sequences.

- While the number of aftershocks increases as the power E^a of the mainshock energy E, the number of foreshocks of type II is independent of E. Thus, the seismicity generated by the ETAS model increases on average according to the inverse Omori law before any earthquake, whatever its magnitude. For foreshocks of type I, the same results hold for large mainshocks while the conditioning on foreshocks of type I to be smaller than their mainshock makes their number increase with E for small and intermediate values of the mainshock size.

- Conditioned on the fact that a foreshock sequence leads to a burst of seismic activity accompanying the mainshock, we find that the foreshock energy distribution is modified upon the approach of the mainshock, and develops a bump in its tail. This result may explain both the often reported decrease in measured b-value before large earthquakes and the smaller b-value obtained for foreshocks compared with other earthquakes.

- In the ETAS model, the modification of the Gutenberg-Richter distribution for foreshocks is shown analytically to take the shape of an additive correction to the standard power law, in which the new term is another power law with exponent $\beta - a$. The amplitude of this additive power law term also exhibits a kind of inverse Omori law acceleration upon the approach to the mainshock, with a different exponent. These predictions are accurately substantiated by our numerical simulations.

- When looking at the spatial distribution of foreshocks in the ETAS model, we find that the foreshocks migrate towards the mainshock as the time increase. This migration is driven by the same mechanism underlying the aftershock diffusion [*Helmstetter and Sornette*, 2002b].

Thus, the ETAS model, which is commonly used to describe aftershock activity, seems sufficient to explain the main properties of foreshock behavior in the real seismicity. Our presentation is organized as follows. In the next section, we define the ETAS model,

recall how the average rate of seismicity can be obtained formally from a Master equation and describe how to deal with fluctuations decorating the average rate. The third section provides the full derivation of the inverse Omori law, first starting with an intuitive presentation followed by a more technical description. Section four contains the derivation of the modification of the distribution of foreshock energies. Section 5 describes the migration of foreshock activity. Section 6 is a discussion of how our analytical and numerical results allows us to rationalize previous empirical observations. In particular, we show that foreshocks are not just statistical creatures but are genuine forerunners of large shocks that can be used to obtain significant prediction gains. Section 7 concludes.

2. Definition of the ETAS model and its master equation for the renormalized Omori law

2.1. Definitions

The ETAS model was introduced by *Kagan and Knopoff* [1981, 1987] and *Ogata* [1988] to describe the temporal and spatial clustering of seismicity and has since been used by many other workers with success to describe real seismicity. Its value stems from the remarkable simplicity of its premises and the small number of assumptions, and from the fact that it has been shown to fit well to seismicity data [*Ogata*, 1988].

Contrary to the usual definition of aftershocks, the ETAS model does not impose an aftershock to have an energy smaller than the mainshock. This way, the same underlying physical mechanism is assumed to describe both foreshocks, aftershocks and mainshocks. The abandon of the ingrained concept (in many seismologists' mind) of the distinction between foreshocks, aftershocks and mainshocks is an important step towards a simplification and towards an understanding of the mechanism underlying earthquake sequences. Ultimately, this parsimonious assumption will be validated or falsified by the comparison of its prediction with empirical data. In particular, the deviations from the predictions derived from this assumption will provide guidelines to enrich the physics.

In order to avoid problems arising from divergences associated with the proliferation of small earthquakes, the ETAS model assumes the existence of a magnitude cut-off m_0, or equivalently an energy cut-off E_0, such that only earthquakes of magnitude $m \geq m_0$ are allowed to give birth to aftershocks larger than m_0, while events of smaller magnitudes are lost for the epidemic dynamics. We refer to [*Helmstetter and Sornette*, 2002a] for a justification of this hypothesis and a discussion of ways to improve this description.

The ETAS model assumes that the seismicity rate (or "bare Omori propagator") at a time between t and $t + dt$, resulting in direct "lineage" (without intermediate events) from an earthquake i that occurred at time t_i, is given by

$$\phi_{E_i}(t - t_i) = \rho(E_i)\ \Psi(t - t_i)\ , \qquad (1)$$

where $\Psi(t)$ is the normalized waiting time density distribution (that we shall take later given by (4) and $\rho(E_i)$ defined by

$$\rho(E_i) = k\ (E_i/E_0)^a \qquad (2)$$

gives the average number of daughters born from a mother with energy $E_i \geq E_0$. This term $\rho(E_i)$ accounts for the fact that large mothers have many more daughters than small mothers because the larger spatial extension of their rupture triggers a larger domain. Expression (2) results in a natural way from the assumption that aftershocks are events influenced by stress transfer mechanisms extending over a space domain proportional to the size of the mainshock rupture [*Helmstetter*, 2003]. Indeed, using the well-established scaling law relating the size of rupture and the domain extension of aftershocks [*Kagan*, 2002] to the release energy (or seismic moment), and assuming a uniform spatial distribution of aftershocks in their domain, expression (2) immediately follows (it still holds if the density of aftershocks is slowly varying or power law decaying with the distance from the mainshock).

The value of the exponent a controls the nature of the seismic activity, that is, the relative role of small compared to large earthquakes. Few studies have measured a in seismicity data [*Yamanaka and Shimazaki*, 1990; *Guo and Ogata*, 1997; *Helmstetter*, 2003]. This parameter a is often found close to the β exponent of the energy distribution defined below in equation (3) [e.g., *Yamanaka and K. Shimazaki*, 1990] or fixed arbitrarily equal to β [e.g., *Kagan and Knopoff*, 1987; *Reasenberg and Jones*, 1989; *Felzer et al.*, 2002]. For a large range of mainshock magnitudes and using a more sophisticated scaling approach, *Helmstetter* [2003] found $a = 0.8\beta$ for the Southern California seismicity. If $a < \beta$, small earthquakes, taken together, trigger more aftershocks than larger earthquakes. In contrast, large earthquakes

dominate earthquake triggering if $a \geq \beta$. This case $a \geq \beta$ has been studied analytically in the framework of the ETAS model by *Sornette and Helmstetter* [2002] and has been shown to eventually lead to a finite time singularity of the seismicity rate. This explosive regime cannot however describe a stationary seismic activity. In this paper, we will therefore consider only the case $a < \beta$.

An additional space-dependence can be added to $\phi_{E_i}(t - t_i)$ [*Helmstetter and Sornette*, 2002b]: when integrated over all space, the prediction of the space-time model retrieves those of the pure time-dependent model. Since we are interested in the inverse Omori law for foreshocks, which is a statement describing only the time-dependence, it is sufficient to use the time-only version of the ETAS model for the theory.

The model is complemented by the Gutenberg-Richter law which states that each aftershock i has an energy $E_i \geq E_0$ chosen according to the density distribution

$$P(E) = \frac{\beta E_0^\beta}{E^{1+\beta}}, \quad \text{with} \quad \beta \simeq 2/3 \ . \tag{3}$$

$P(E)$ is normalized $\int_{E_0}^{\infty} dE \ P(E) = 1$.

In view of the empirical observations that the observed rate of aftershocks decays as a power law of the time since the mainshock, it is natural to choose the "bare" modified Omori law (or the normalized waiting time distribution between events) $\Psi(t - t_i)$ in (1) also as a power law

$$\Psi(t - t_i) = \frac{\theta \ c^\theta}{(t - t_i + c)^{1+\theta}} \ . \tag{4}$$

$\Psi(t-t_i)$ is the rate of daughters of the first generation born at time $t-t_i$ from the mother-mainshock. Here, c provides an "ultra-violet" cut-off which ensures the finiteness of the number of aftershocks at early times. It is important to recognize that the observed aftershock decay rate may be different from $\Psi(t - t_i)$ due to the effect of aftershocks of aftershocks, and so on [*Sornette and Sornette*, 1999; *Helmstetter and Sornette*, 2002a]

The ETAS model is a "branching" point-process [*Harris*, 1963; *Daley and Vere-Jones*, 1988] controlled by the key parameter n defined as the average number (or "branching ratio") of daughter-earthquakes created per mother-event, summed over all times and averaged over all possible energies. This branching ratio n is defined as the following integral

$$n \equiv \int_0^\infty dt \int_{E_0}^\infty dE \ P(E) \ \phi_E(t) \ . \tag{5}$$

The double integral in (5) converges if $\theta > 0$ and $a < \beta$. In this case, n has a finite value

$$n = \frac{k\beta}{\beta - a} \ , \tag{6}$$

obtained by using the separability of the two integrals in (5). The normal regime corresponds to the subcritical case $n < 1$ for which the seismicity rate decays after a mainshock to a constant background (in the case of a steady-state source) decorated by fluctuations in the seismic rate.

The total rate of seismicity $\lambda(t)$ at time t is given by

$$\lambda(t) = s(t) + \sum_{i \ | \ t_i \leq t} \phi_{E_i}(t - t_i) \tag{7}$$

where $\phi_{E_i}(t-t_i)$ is defined by (1). The sum $\sum_{i \ | \ t_i \leq t}$ is performed over all events that occurred at time $t_i \leq t$, where E_i is the energy of the earthquake that occurred at t_i. $s(t)$ is often taken as a stationary Poisson background stemming from plate tectonics and provides a driving source to the process. The second term in the right-hand-side of expression (7) is nothing but the sum of (1) over all events preceding time t.

Note that there are three sources of stochasticity underlying the dynamics of $\lambda(t)$: (i) the source term $s(t)$ often taken as Poissonian, (ii) the random occurrences of preceding earthquakes defining the time sequence $\{t_i\}$ and (iii) the draw of the energy of each event according to the distribution $P(E)$ given by (3). Knowing the seismic rate $\lambda(t)$ at time t, the time of the following event is then determined according to a non-stationary Poisson process of conditional intensity $\lambda(t)$, and its magnitude is chosen according to the Gutenberg-Richter distribution (3).

2.2. The Master equation for the average seismicity rate

It is useful to rewrite expression (7) formally as

$$\lambda(t) = s(t) + \int_{-\infty}^{t} d\tau \int_{E_0}^{+\infty} dE \ \phi_E(t - \tau) \sum_{i \ | \ t_i \leq t} \delta(E - E_i) \ \delta(\tau - t_i) \ , \tag{8}$$

where $\delta(u)$ is the Dirac distribution. Taking the expectation of (8) over all possible statistical scenarios (so-called ensemble average), and assuming the separability in time and magnitude, we obtain the following Master equation for the first moment or statistical average $N(t)$ of $\lambda(t)$ [*Helmstetter and Sornette*, 2002a]

$$N(t) = \mu + \int_{-\infty}^{t} d\tau \ \phi(t-\tau) \ N(\tau) \ , \qquad (9)$$

where μ is the expectation of the source term $s(t)$ and

$$\phi(t) \equiv \int_{E_0}^{\infty} dE' \ P(E') \ \phi_{E'}(t) \ . \qquad (10)$$

By virtue of (6), $\int_0^\infty \phi(t)dt = n$. We have used the definitions

$$N(t) = \langle \lambda(t) \rangle = \langle \sum_{t_i \leq t} \delta(t-t_i) \rangle \ , \qquad (11)$$

and

$$P(E) = \langle \delta(E-E_i) \rangle \ , \qquad (12)$$

where the brackets $\langle . \rangle$ denotes the ensemble average. The average is performed over different statistical responses to the same source term $s(t)$, where $s(t)$ can be arbitrary. $N(t)dt$ is the average number of events occurring between t and $t+dt$ of any possible energy.

The essential approximation used to derive (9) is that

$$\langle \rho(E_i)\delta(E-E_i) \ \delta(\tau-t_i) \rangle = \langle \rho(E_i)\delta(E-E_i) \rangle \ \langle \delta(\tau-t_i) \rangle \qquad (13)$$

in (8). In words, the fluctuations of the earthquake energies can be considered to be decoupled from those of the seismic rate. This approximation is valid for $a < \beta/2$, for which the random variable $\rho(E_i)$ has a finite variance. In this case, any coupling between the fluctuations of the earthquake energies and the instantaneous seismic rate provides only sub-dominant corrections to the equation (9). For $a > \beta/2$, the variance of $\rho(E_i)$ is mathematically infinite or undefined as $\rho(E_i)$ is distributed according to a power law with exponent $\beta/a < 2$ (see chapter 4.4 of [*Sornette*, 2000]). In this case, the Master equation (9) is not completely correct as an additional term must be included to account for the dominating effect of the dependence between the fluctuations of earthquake energies and the instantaneous seismic rate.

Equation (9) is a linear self-consistent integral equation. In the presence of a stationary source of average level μ, the average seismicity in the sub-critical regime is therefore

$$\langle N \rangle = \frac{\mu}{1-n} \ . \qquad (14)$$

This result (14) shows that the effect of the cascade of aftershocks of aftershocks and so on is to renormalize the average background seismicity $\langle s \rangle$ to a significantly higher level, the closer n is to the critical value 1.

In order to solve for $N(t)$ in the general case, it is convenient to introduce the Green function or "dressed propagator" $K(t)$ defined as the solution of (9) for the case where the source term is a delta function centered at the origin of time corresponding to a single mainshock:

$$K(t) = \delta(t) + \int_0^t d\tau \ \phi(t-\tau) \ K(\tau) \ . \qquad (15)$$

Physically, $K(t)$ is nothing but the "renormalized" Omori law quantifying the fact that the event at time 0 started a sequence of aftershocks which can themselves trigger secondary aftershocks and so on. The cumulative effect of all the possible branching paths of activity gives rise to the net seismic activity $K(t)$ triggered by the initial event at $t = 0$. Thus, the decay rate of aftershocks following a mainshock recorded in a given earthquake catalog is described by $K(t)$, while $\Psi(t)$ defined by (4) is a priori unobservable (see however [*Helmstetter and Sornette*, 2002a]).

This remark is important because it turns out that the renormalized Omori law $K(t)$ may be very different from the bare Omori law $\Psi(t-t_i)$, because of the effect of the cascade of secondary, tertiary, ..., events triggered by any single event. The behavior of the average renormalized Omori law $K(t)$ has been fully classified in [*Helmstetter and Sornette*, 2002a] (see also [*Sornette and Sornette*, 1999]): with a single value of the exponent $1+\theta$ of the "bare" propagator $\Psi(t) \sim 1/t^{1+\theta}$ defined in (4), one obtains a continuum of apparent exponents for the global rate of aftershocks. This result may account for the observed variability of Omori exponent p in the range $0.5-1.5$ or beyond, as reported by many workers [*Utsu et al.*, 1995]. Indeed, the general solution of (15) in the subcritical regime $n < 1$ is

$$\begin{aligned} K(t) &\sim 1/t^{1-\theta} \ , \text{ for } \ c < t < t^* \ , \\ K(t) &\sim 1/t^{1+\theta} \ , \text{ for } \ t > t^* \ , \end{aligned} \qquad (16)$$

where

$$t^* \approx c(1-n)^{-1/\theta} \ . \tag{17}$$

Thus, in practice, the apparent p exponent can be found anywhere between $1-\theta$ and $1+\theta$. This behavior (16) is valid for $a < \beta/2$ for which, as we explained already, the fluctuations of the earthquake energies can be considered to be decoupled from those of the seismic rate.

In the case $a > \beta/2$, this approximation is no more valid and the problem is considerably more difficult due to the coupling between the fluctuations in the sequence of earthquake energies and the seismic rate. We have not been able to derive the detailed solution of the problem in this regime but nevertheless can predict that the apparent exponent for the dressed propagator $K(t)$ should change continuously from $1-\theta$ to $1+\theta$ as a increases towards β from below. The argument goes as follows. Starting from (8), it is clear that the larger a is, the larger is the dependence between the times of occurrences contributing to the sum over $\delta(\tau - t_i)$ and the realizations of corresponding earthquake energies contributing to the sum over $\delta(E - E_i)$. This is due to the fact that very large earthquakes trigger many more aftershocks for large a, whose energies influence subsequently the time of occurrences of following earthquakes, and so on. The larger is the number of triggered events per shock, the more intrically intertwined are the times of occurrence and energies of subsequent earthquakes.

We have not been able to derive a full and rigorous analytical treatment of this dependence, yet. Nevertheless, it is possible to predict the major effect of this dependence by the following argument. Consider two random variables X and Y, which are (linearly) correlated. Such a linear correlation is equivalent to the existence of a linear regression of one variable with respect to the other: $Y = \gamma X + x$, where γ is non-random and is simply related to the correlation coefficient between X and Y and x is an idiosyncratic noise uncorrelated with X. Then,

$$\langle XY \rangle = \gamma \langle X^2 \rangle + \langle X \rangle \ \langle x \rangle \ , \tag{18}$$

which means that the covariance of X and Y contains a term proportional to the variance of X.

Let us now apply this simple model to the effect of the dependence between $X \equiv \delta(\tau - t_i)$ and $Y \equiv \rho(E_i)\delta(E - E_i)$ in the earthquake cascade process. We propose to take into account this dependence by the following ansatz, which corrects (13), based on a description capturing the dependence through the second-order moment, that is, their covariance:

$$\langle \rho(E_i)\delta(E - E_i) \ \delta(\tau - t_i) \rangle \approx$$

$$\langle \rho(E_i)\delta(E - E_i) \rangle \ \langle \delta(\tau - t_i) \rangle + \gamma(a) \langle [\delta(\tau - t_i)]^2 \rangle \ , \tag{19}$$

where $\gamma(a) = 0$ for $a < \beta/2$ and increases with $a > \beta/2$. The quadratic term just expresses the dependence between $\rho(E_i)\delta(E - E_i)$ and $\delta(\tau - t_i)$, i.e., $\rho(E_i)\delta(E - E_i)$ has a contribution proportional to $\delta(\tau - t_i)$ as in (18): the mechanism leading to the quadratic term $\langle X^2 \rangle$ is at the source of $[\delta(\tau - t_i)]^2$ in (19). This new contribution leads to a modification of (15) according to

$$K(t) \sim \int_0^t d\tau \ \phi(t-\tau) \ K(\tau) + \gamma(a) \int_0^t d\tau \ \phi(t-\tau) \ [K(\tau)]^2 \ . \tag{20}$$

Dropping the second term in the right-hand-side of (20) recovers (15). Dropping the first term in the right-hand-side of (20) yields the announced result $K(t) \propto 1/t^{1+\theta}$ even in the regime $t < t^*$. We should thus expect a cross-over from $K(t) \propto 1/t^{1-\theta}$ to $K(t) \propto 1/t^{1+\theta}$ as a increases from $\beta/2$ to β. This prediction is verified accurately by our numerical simulations.

Once we know the full (ensemble average) seismic response $K(t)$ from a single event, the complete solution of (9) for the average seismic rate $N(t)$ under the action of the general source term $s(t)$ is

$$N(t) = \int_{-\infty}^t d\tau \ s(\tau) \ K(t - \tau) \ . \tag{21}$$

Expression (21) is nothing but the theorem of Green functions for linear equations with source terms [*Morse and Feshbach*, 1953]. Expression (21) reflects the intuitive fact that the total seismic activity at time t is the sum of the contributions of all the external sources at all earlier times τ which convey their influence up to time t via the "dressed propagator" (or renormalized Omori law) $K(t - \tau)$. $K(t - \tau)$ is the relevant kernel quantifying the influence of each source $s(\tau)$ because it takes into account all possible paths of seismicity from τ to t triggered by each specific source.

2.3. Deviations from the average seismicity rate

Similarly to the definition (15) of the average renormalized propagator $K(t)$, let us introduce the stochastic propagator $\kappa(t)$, defined as the solution

of (7) or (8) for the source term $s(t) = \delta(t)$. The propagator $\kappa(t)$ is thus the seismicity rate initiated by a single earthquake at the origin of times, which takes into account the specific sequence of generated earthquakes. Since the earthquakes are generated according to a probabilistic (generalized Poisson) process, repeating the history leads in general to different realizations. $\kappa(t)$ is thus fundamentally realization-specific and there are as many different $\kappa(t)$'s as there are different earthquake sequences. In other words, $\kappa(t)$ is a stochastic function. Obviously, $\langle \kappa(t) \rangle \equiv K(t)$, that is, its ensemble average retrieves the average renormalized propagator.

From the structure of (7) or (8) which are linear sums over events, an expression similar to (21) can be written for the non-average seismic rate with an arbitrary source term $s(t)$:

$$\lambda(t) = \int_{-\infty}^{t} d\tau \; s(\tau) \; \kappa_{\{\tau\}}(t-\tau) \; , \qquad (22)$$

where the subscript $\{\tau\}$ in the stochastic kernel $\kappa_{\{\tau\}}(t-\tau)$ captures the fact that there is a different stochastic realization of κ for each successive source. Taking the ensemble average of (22) recovers (21). The difference between the stochastic kernel $\kappa_{\{\tau\}}(t-\tau)$, the local propagator $\phi_E(\tau)$ and the renormalized propagator $K(\tau)$ is illustrated on Figure 1 for a numerical simulation of the ETAS model.

We show in the Appendix A that $\lambda(t)$ can be expressed as

$$\lambda(t) = N(t) + \int_{-\infty}^{t} d\tau \; \eta(\tau) \; K(t-\tau) \; , \qquad (23)$$

where $\eta(\tau)$ is a stationary noise which can be suitably defined. This is the case because the fluctuations $\delta P(E)$ of the Gutenberg-Richter law and of the source $s(t)$ are stationary processes, and because the fluctuations of $\delta\kappa$ are proportional to $K(t)$. The expression of $\eta(\tau)$ can be determined explicitly in the case where the fluctuations of the energy distribution $P(E)$ dominate the fluctuations of the seismicity rate $\kappa(\tau)$ (see Appendix A).

3. Derivation of the inverse Omori law and consequences

3.1. Synthesis of the results

The normal regime in the ETAS model corresponds to the subcritical case $n < 1$ for which the seismicity rate decays on average after a mainshock to a constant background (in the case of a steady-state source) decorated by fluctuations. How is it then possible in this framework to get an accelerating seismicity preceding a large event? Conceptually, the answer lies in the fact that when one defines a mainshock and its foreshocks, one introduces automatically a conditioning (in the sense of the theory of probability) in the earthquake statistics. As we shall see, this conditioning means that specific precursors and aftershocks must precede and follow a large event. In other words, conditioned on the observation of a large event, the sequence of events preceding it cannot be arbitrary. We show below that it in fact follows the inverse Omori law in an average statistical sense. Figure 2 presents typical realizations of foreshock and aftershock sequences in the ETAS model as well as the direct and inverse Omori law evaluated by averaging over many realizations. The deceleration of the aftershock activity is clearly observed for each individual sequence as well as in their average. Going to backward time to compare with foreshocks, the acceleration of aftershock seismicity when approaching the main event is clearly visible for each sequence. In contrast, the acceleration of foreshock activity (in forward time) is only observable for the ensemble average while each realization exhibits large fluctuations with no clearly visible acceleration. This stresses the fact that the inverse Omori law is a statistical statement, which has a low probability to be observed in any specific sequence.

Intuitively, it is clear that within the ETAS model, an event is more likely to occur after an increase both in seismicity rate and in magnitudes of the earthquakes, so that this increase of seismicity can trigger an event with a non-negligible probability. Indeed, within the ETAS model, all events are the result of the sum of the background seismicity (due to tectonic forces) and of all other earthquakes that can trigger their aftershocks.

How does the condition that an earthquake sequence ends at a mainshock impact on the seismicity prior to that mainshock? How does this condition create the inverse Omori law? Since earthquake magnitudes are independently drawn from the Gutenberg-Richter law, the statistical qualification of a mainshock, that we place without loss of generality at the origin of time, corresponds to imposing an anomalous burst of seismic activity $\lambda(0) = \langle N \rangle + \lambda_0$ at $t = 0$ above its average level $\langle N \rangle$ given by (14). For the study of type II foreshocks (as defined in the intro-

duction), we do not constrain the mainshock to be larger than the seismicity before and after this mainshock. For large mainshock magnitudes, relaxing this hypothesis will not change the results derived below.

The question then translates into what is the path taken by the noise $\eta(\tau)$ in (23) for $-\infty < \tau < 0$ that may give rise to this burst λ_0 of activity. The solution is obtained from the key concept that the set of $\eta(\tau)$'s for $-\infty < \tau < 0$ is biased by the existence of the conditioning, i.e., by the large value of $\lambda(0) = \langle N \rangle + \lambda_0$ at $t = 0$. This does not mean that there is an unconditional bias. Rather, the existence of a mainshock requires that a specific sequence of noise realizations must have taken place to ensure its existence. This idea is similar to the well-known result that an unbiased random walk $W(t)$ with unconditional Gaussian increments with zero means sees its position take a non-zero expectation

$$\langle W(\tau) \rangle|_c = [W(t) - W(0)] \, \frac{\tau}{t} \, , \qquad (24)$$

if one knows the beginning $W(0)$ and the end $W(t)$ position of the random walk, while the unconditional expectation $\langle W(\tau) \rangle$ is identically zero. Similarly, the conditional increment from τ to $\tau + d\tau$ of this random walk become not non-zero and equal to (in non-rigorous notation)

$$d\tau \, \frac{W(t) - W(0)}{t} \, , \qquad (25)$$

in contrast with the zero value of the unconditional increments.

In the ETAS model which is a marked point process, the main source of the noise on $\lambda(t)$ is coming from the "marks", that is, the energies drawn for each earthquake from the Gutenberg-Richter power law distribution (3). Expression (2) shows that the amplitude η_τ of the fluctuations in the seismic rate is proportional to E_τ^a, where E_τ is the energy of a mother-earthquake occurring at time τ. Since the energies are distributed according to the power law (3) with exponent β, $\eta_\tau \propto E_\tau^a$ is distributed according to a power law with exponent $m = \beta/a$ (see for instance chapter 4.4 of [*Sornette*, 2000]).

We first study the subcritical regime $n < 1$ for times $t_c - t < t^*$, where t^* is defined by (17). Two cases must then be considered.

- For $a < \beta/2$, $m > 2$, the variance and covariance of the noise η_τ exist and one can use conditional covariances to calculate conditional expectations. We show below that the inverse Omori law takes the form

$$\mathrm{E}[\lambda(t)|\lambda_0] \propto \frac{\lambda_0}{(t_c - t)^{1-2\theta}} \, , \qquad (26)$$

that is, $p' = 1 - 2\theta$.

- for $a \geq \beta/2$, $m = \beta/a \leq 2$ and the variance and covariance of η_τ do not exist: one needs a special treatment based on stable distributions. In this case, neglecting the coupling between the fluctuations in the earthquake energies and the seismic rate, we find that the inverse Omori law takes the form

$$\mathrm{E}[\lambda(t)|\lambda_0] \propto \frac{\lambda_0}{(t_c - t)^{1-m\theta}} \, . \qquad (27)$$

Taking into account the dependence between the fluctuations in the earthquake energies and the seismic rate, the exponent p' progressively increases from $1 - 2\theta$ towards the value $1 + \theta$ of the bare propagator as a goes from $\beta/2$ to β (see Figure 6). The increase of p' is thus faster than the dependence $1 - m\theta$ predicted by (27).

In the large times limit $t_c - t > t^*$ (far from the mainshock) of the subcritical regime, we also obtain an inverse Omori law which takes the form

$$\mathrm{E}[\lambda(t)|\lambda_0] \propto \frac{\lambda_0}{(t_c - t)^{1+\theta}} \, , \qquad \text{for} \quad a < \beta/2 \qquad (28)$$

and

$$\mathrm{E}[\lambda(t)|\lambda_0] \propto \frac{\lambda_0}{(t_c - t)^{1+(m-1)\theta}} \, , \qquad \text{for} \quad \beta/2 \leq a \leq \beta \, . \qquad (29)$$

The direct and inverse Omori laws are clearly observed in numerical simulations of the ETAS model, when stacking many sequences of foreshocks and aftershocks, for various mainshock magnitudes (Figures 3 and 4). Our main result shown in Figure 3 is that, due to conditioning, the inverse Omori law is *different* from the direct Omori law, in that the exponent p' of the inverse Omori law is in general smaller than the exponent p of the direct Omori law. Another fundamental difference between aftershocks and foreshocks found in the ETAS model is that the number of aftershocks increases as a power E^a of the mainshock energy E as given by (2), whereas the number of foreshocks of type II is independent of the mainshock energy (see Figures 3 and 4). Because in the ETAS model the magnitude of each event is independent of the magnitude of the triggering events,

and of the previous seismicity, the rate of seismicity increases on average according to the inverse Omori law before any earthquake, whatever its magnitude. The number of foreshocks of type I increases with the mainshock magnitude, for small and intermediate mainshock magnitudes and saturates to the level of foreshocks of type II for large mainshocks because the selection/condition acting of those defined foreshocks becomes less and less severe as the magnitude of the mainshock increases (see Figure 5). The conditioning that foreshocks of type I must be smaller than their mainshock induces an apparent increase of the Omori exponent p' as the mainshock magnitude decreases. The predictions (16) and (26) on the p and p'-value of type II foreshocks are well-verified by numerical simulations of the ETAS model up to $a/\beta = 0.5$, as presented on Figure 6. However, for $a/\beta > 0.5$, both p and p' are found larger than predicted by (16) and (27) respectively, due to the coupling between the fluctuations in the earthquake energies and those of the seismic rate. This coupling occurs because the variance of the number $\rho(E)$ of direct aftershocks of an earthquake of energy E is unbounded for $a > \beta/2$, leading to strong burst of seismic activity coupled with strong fluctuations of the earthquake energies. In this regime, expression (20) shows that p changes continuously between $1-\theta$ for $a/\beta = 0.5$ to $1+\theta$ for $a = \beta$ in good agreement with the results of the numerical simulations. In this case $a \geq \beta/2$, the exponent p' is also observed to increase between $p' = 1-2\theta$ for $a = \beta/2$ to $p' = 1+\theta$ for $a = \beta$, as predicted below.

The dissymetry between the inverse Omori law for foreshocks and the direct Omori law (16) for aftershocks stems from the fact that, for foreshocks, one observes a seismic rate conditional on a large rate at the time t_c of the mainshock while, for the aftershocks, one observes the direct response $K(t)$ to a single large shock. The later effect stems from the term $\rho(E)$ given by (2) in the bare Omori propagator which ensures that a mainshock with a large magnitude triggers aftershocks which dominates overwhelmingly the seismic activity. In the special case where one take the exponent $a = 0$ in (2), a mainshock of large magnitude has no more daughters than any other earthquake. As a consequence, the observed Omori law stems from the same mechanism as for the foreshock and the increasing foreshock activity (26) gives the same parametric form for the aftershock decay, with $t_c - t$ replaced by $t - t_c$ (this is for instance obtained through the Laplace transform of the seismic rate). This gives the exponent $p = p' = 1-2\theta$ for $a = 0$ as for the foreshocks, but the number of aftershocks is still larger than the number of foreshocks. This result is born out by our numerical simulations (not shown).

These results and the derivations of the inverse Omori law make clear that mainshocks are more than just the aftershocks of their foreshocks, as sometimes suggested [*Shaw*, 1993; *Jones et al.*, 1999]. The key concept is that all earthquakes are preceded by some seismic activity and may be seen as the result of this seismic activity. However, on average, this seismic activity must increase to be compatible statistically with the occurrence of the main shock: this is an unavoidable statistical certainty with the ETAS model, that we derive below. The inverse Omori law is fundamentally a conditional statistical law which derives from a double renormalization process: (1) the renormalization from the bare Omori propagator $\Psi(t)$ defined by (4) into the renormalized or dressed propagator $K(t)$ and (2) the conditioning of the fluctuations in seismic activity upon a large seismic activity associated with the mainshock. In summary, we can state that mainshocks are aftershocks of conditional foreshocks. We stress again that the statistical nature of foreshocks does not imply that there is no information in foreshocks on future large earthquakes. As discussed below, in the ETAS model, foreshocks are forerunners of large shocks.

3.2. The inverse Omori law $\sim 1/t^{1-2\theta}$ for $a < \beta/2$

Let us call $X(t) = \lambda(t) - N(t)$ given by (23) and $Y = \lambda(0) - N(0)$. It is a standard result of stochastic processes with finite variance and covariance that the expectation of $X(t)$ conditioned on $Y = \lambda_0$ is given by [*Jacod and Shiryaev*, 1987]

$$\mathrm{E}[X(t)|Y=\lambda_0] = \lambda_0 \, \frac{\mathrm{Cov}(X(t),Y)}{\mathrm{E}[Y^2]} \, , \qquad (30)$$

where $\mathrm{E}[Y^2]$ denotes the expectation of Y^2 and $\mathrm{Cov}(X(t),Y)$ is the covariance of X and Y. Expression (30) recovers the obvious result that $\mathrm{E}[X(t)|Y=\lambda_0] = 0$ if X and Y are uncorrelated.

Using the form (23) for $X(t) = \lambda(t) - N(t)$ and the fact that X has a finite variance, we obtain

$$\mathrm{Cov}(X(t),Y) = \int_{-\infty}^{t} d\tau \int_{-\infty}^{0} d\tau' \; K(t-\tau) \; K(-\tau) \; \mathrm{Cov}[\eta(\tau)\eta(\tau')]. \qquad (31)$$

For a dependence structure of $\eta(t)$ falling much faster than the kernel $K(t)$, the leading behavior of $\mathrm{Cov}(X(t), Y)$ is obtained by taking the limit $\mathrm{Cov}(\eta(\tau), \eta(\tau')) = \delta(\tau - \tau')$. This yields

$$\mathrm{Cov}(X(t), Y) = \int_{-\infty}^{t} d\tau \; K(t-\tau) \; K(-\tau) \; , \qquad (32)$$

and

$$\mathrm{E}[Y^2] = \int_{-\infty}^{0} d\tau \; [K(-\tau)]^2 \; . \qquad (33)$$

$\mathrm{E}[Y^2]$ is thus a constant while, for $|t| < t^*$ where t^* is defined in (17), $\mathrm{Cov}(X(t), Y) \sim 1/|t|^{1-2\theta}$. Generalizing to a mainshock occurring at an arbitrary time t_c, this yields the inverse Omori law

$$\mathrm{E}[\lambda(t)|\lambda(t_c) = \langle N \rangle + \lambda_0] = \langle N \rangle + C \frac{\lambda_0}{(t_c - t)^{1-2\theta}} \; , \qquad (34)$$

where C is a positive numerical constant.

Expression (34) predicts an inverse Omori law for foreshocks in the form of an average acceleration of seismicity proportional to $1/(t_c - t)^{p'}$ with the inverse Omori exponent $p' = 1 - 2\theta$, prior to a mainshock. This exponent p' is smaller than the exponent $p = 1 - \theta$ of the renormalized propagator $K(t)$ describing the direct Omori law for aftershocks. This prediction is well-verified by numerical simulations of the ETAS model shown in Figure 3.

As we pointed out in the introduction, *Shaw* [1993] derived the relationship $p' = 2p - 1$, which yields $p' = 1 - 2\theta$ for $p = 1 - \theta$, based on a clever interestingly incorrect reasoning that we now clarify. Actually, there are two ways of viewing his argument. The most straightforward one used by Shaw himself consists in considering a single aftershock sequence starting at time 0 from a large mainshock. Let us consider two aftershocks at time $t - \tau$ and t. Forgetting any constraint on the energies, the earthquake at time $t - \tau$ can be viewed as a foreshock of the earthquake at time t. Summing over all possible positions of these two earthquakes at fixed time separation τ then amounts to constructing a kind of foreshock count which obeys the equation

$$\int_{0}^{+\infty} dt \; K(t-\tau) \; K(t) \; , \qquad (35)$$

where $K(t)$ is the number of aftershocks at time t. This integral (35) recovers equation (12) of [*Shaw*, 1993]. If $K(t) \sim 1/t^p$, this integral predicts a dependence $1/\tau^{2p-1}$ for the effective foreshock activity. This derivation shows that the prediction $p' = 2p - 1$ results solely from the counting of pairs at fixed time intervals in an aftershock sequence. It is a pure product of the counting process.

We can also view this result from the point of view of the ETAS model. In the language of the ETAS model, Shaw's formula (12) uses the concept that a mainshock is an aftershock of a cascade of aftershocks, themselves deriving from an initial event. This idea implies that the probability for a mainshock to occur is the sum over all possible time occurrences of the product of (i) the probability for an aftershock to be triggered by the initial event and (ii) the probability that this aftershock triggers its own aftershock at the time of the mainshock. Shaw uses (what corresponds to) the dressed propagator $K(t)$ for the first probability. He also assumes that the rate of mainshocks deriving from an aftershock of the initial event is proportional to $K(t)$. However, from our previous studies [*Sornette and Sornette*, 1999; *Helmstetter and Sornette*, 2002a] and the present work, one can see that this corresponds to an illicit double counting or double renormalization. This danger of double counting is illustrated by comparing the formulas (9, 15) with (21). Either the direct tectonic source of seismicity $s(t)$ impacts the future seismicity by a weight given by the renormalized or dressed propagator as in (21). Or we can forget about the tectonic source term $s(t)$, we only record all past seismic activity (all sources and all triggered events) as in (9, 15), but then the impact of all past seismicity on future seismicity is weighted by the bare propagator. These two view points are completely equivalent and are two alternative expressions of the Green theorem. What is then the reason for the correct $1/t^{1-2\theta}$ inverse Omori law derived by *Shaw* [1993]? It turns out that his (erroneous) double counting recovers the mathematical form resulting from the effect of the conditioning of past seismicity leading to $s(t) \sim K(t)$ valid for $a \leq \beta/2$ as derived below in (39). Indeed, inserting $s(t) \sim K(t)$ in (21) retrieves the correct prediction $1/t^{1-2\theta}$ for the inverse Omori law. This proportionality $s(t) \sim K(t)$ is physically at the origin of (32) at the origin itself of the inverse Omori law. In other words, Shaw obtains the correct result (35) by incorrect double counting while the correct way to get (35) is that the mainshock is conditional on a specific average trajectory of past seismicity captured by $s(t) \sim K(t)$. In addition to provide a more correct reasoning, our approach al-

lows one to explore the role of different parameter regimes and, in particular, to analyze the failure of the argument for $a > \beta/2$, as already explained.

3.3. The inverse Omori law $\sim 1/t^{1-\theta\beta/a}$ for $a \geq \beta/2$

Expression (23) defines the fluctuating part $X(t) = \lambda(t) - N(t)$ of the seismic rate as a sum of random variables $\eta(\tau)$ with power law distributions weighted by the kernel $K(t-\tau)$. These random variables $\eta(\tau)$, which are mainly dominated by the fluctuations in event magnitudes but also receive contributions from the intermittent seismic rate, are conditioned by the realization of a large seismicity rate

$$X(0) = \lambda_0 = \int_{-\infty}^{0} d\tau \ \eta(\tau) \ K(-\tau) \ , \tag{36}$$

which is the correct statistical implementation of the condition of the existence of a large shock at $t = 0$. Since the conditioning is performed on $X(0)$, that is, upon the full set of noise realizations acting up to time $t = 0$, the corresponding conditional noises up to time $t < 0$ contribute all to $\mathrm{E}[X(t)|X(0) = \lambda_0]_{t<0}$ by their conditional expectations as

$$\mathrm{E}[X(t)|X(0) = \lambda_0]_{t<0} = \int_{-\infty}^{t} d\tau \ \mathrm{E}[\eta(\tau)|X(0)] \ K(t-\tau) \ . \tag{37}$$

In Appendix B, it is shown that, for identically independently distributed random variables x_i distributed according to a power law with exponent $m = \beta/a \leq 2$ and entering the sum

$$S_N = \sum_{i=1}^{N} K_i x_i \tag{38}$$

where the K_i are arbitrary positive weights, the expectation $\mathrm{E}[x_i|S_N]$ of x_i conditioned on the existence of a large realization of S_N is given by

$$\mathrm{E}[x_i|S_N] \propto S_N \ K_i^{m-1} \ . \tag{39}$$

To apply this result to (37), it is convenient to discretize it. Some care should however be exercised in this discretization (1) to account for the expected power law acceleration of $\mathrm{E}[X(t)|X(0) = \lambda_0]$ up to $t = 0$ and (2) to discretize correctly the random noise. We thus write

$$\int_{-\infty}^{0} d\tau \ \eta(\tau) \ K(-\tau) \approx \sum_{\tau_i<0} \int_{\tau_i}^{\tau_{i+1}} d\tau \ \eta(\tau) \ K(-\tau)$$

$$\sim \sum_{\tau_i<0} (\tau_{i+1} - \tau_i) \ K(-\tau_i) \ x_i \ , \tag{40}$$

where $x_i \sim \eta_i(\tau_{i+1} - \tau_i)$ is the stationary discrete noise distributed according to a power law distribution with exponent $m = \beta/a$. The factor $(\tau_{i+1} - \tau_i) \propto |\tau_i|$ in front of the kernel $K(-\tau_i)$ is needed to regularize the discretization in the presence of the power law acceleration up to time 0. In the notation of Appendix B, $(\tau_{i+1} - \tau_i) \ K(-\tau_i) \propto |\tau_i| \ K(-\tau_i) \sim 1/|\tau_i|^{-\theta}$ plays the role of K_i. We also need an additional factor $(\tau_{i+1} - \tau_i)$ to obtain a regularized noise term: thus, $\eta_i(\tau_{i+1} - \tau_i) \propto \eta_i|\tau_i|$ plays the role of x_i. This discretization procedure recovers the results obtained by using (30) and the variance and covariance of the continuous integrals for the case $a < \beta/2$ where they are defined. Note that the last expression in equation (40) does not keep track of the dimensions as we are only able to obtain the leading scaling behavior in the discretization scheme.

Using (39), we thus obtain $\mathrm{E}[\eta_i|\tau_i| \ |X(0) = \lambda_0] \propto \frac{\lambda_0}{|\tau_i|^{-\theta(m-1)}}$ and thus

$$\mathrm{E}[\eta_i|X(0) = \lambda_0] \propto \frac{\lambda_0}{|\tau_i|^{1-\theta(m-1)}} \ . \tag{41}$$

Similarly to (40), the discrete equivalent to (37) reads

$$\begin{aligned} &\mathrm{E}[X(t)|X(0) = \lambda_0]_{t<0} \qquad (42)\\ &\approx \sum_{\tau_i<t} (\tau_{i+1} - \tau_i) \ K(t-\tau_i) \ \mathrm{E}[\eta_i|\tau_i| \ |X(0) = \lambda_0] \\ &\sim \int_{-\infty}^{t} d\tau \ \frac{1}{|t-\tau|^{1-\theta}} \ \frac{\lambda_0}{|\tau|^{1-\theta(m-1)}} \sim \frac{\lambda_0}{|t|^{1-m\theta}} \ , \end{aligned}$$

where we have re-introduced the factors $\tau_{i+1} - \tau_i$ to reverse to the continuous integral formulation and have use the definition $m = \beta/a$. Expression (42) gives the inverse Omori law

$$\mathrm{E}[X(t)|X(t_c) = \lambda_0]_{t<0} \propto \frac{\lambda_0}{(t_c - t)^{1-\theta\beta/a}} \tag{43}$$

for foreshock activity prior to a mainshock occurring at time t_c. Note that the border case $m = \beta/a = 2$ recovers our previous result (34) as it should.

The problem is that this derivation does not take into account the dependence between the fluctuations in the earthquake energies and the seismic rate, which become prominent precisely in this regime $\beta/2 \leq a \leq \beta$. We have not been able yet to fully solve this problem for arbitrary values a but can nevertheless predict

that (43) must be replaced by

$$\mathrm{E}[X(t)|X(0)=\lambda_0]_{t<0} \propto \frac{\lambda_0}{|t|^{1+\theta}} \ , \quad \text{for} \ \ a \to \beta \ . \ (44)$$

We follow step by step the reasoning from expression (37) to (42), with the following modifications imposed by the regime $\beta/2 \leq a \leq \beta$.

1. The conditional expectations given by (39) must be progressively changed into $\mathrm{E}[x_i|S_N] \propto S_N \, K_i$ as $a \to \beta$, due to the coupling between energy and seismic rate fluctuations (leading to (19) via the mechanism (18)). Indeed, the coupling between energy and seismic rate fluctuations gives rise to the dependence $\mathrm{E}[x_i|S_N] \propto K_i$ which becomes dominant over the conditional expectations given by (39) for $m < 2$.

2. As shown with (20), the dependence between the fluctuations in the earthquake energies and the seismic rate leads to change $K(t) \propto 1/t^{1-\theta}$ into $K(t) \propto 1/t^{1+\theta}$ as $a \to \beta$ even in the regime $t < t^*$.

This leads finally to changing expressing (42) into

$$\mathrm{E}[X(t)|X(0)] \sim \int_{-\infty}^{t} d\tau \ \frac{1}{|t-\tau+c|^{1+\theta}} \ \frac{\lambda_0}{|\tau|^{1+\theta}} \ , \ (45)$$

where we have re-introduced the regularization constant c to ensure convergence for $\tau \to t$. Taking into account the contribution $\propto t^\theta$ at this upper bound t of the integrand $\propto 1/|t-\tau+c|^{1+\theta}$, we finally get (44). This result is verified numerically in Figure 6.

3.4. The inverse Omori law in the regime $t_c - t > t^*$

The inverse Omori laws derived in the two preceding sections are valid for $t_c - t < t^*$, that is, sufficiently close to the mainshock. A similar inverse Omori law is also obtained for $t_c - t > t^*$. In this goal, we use (16) showing that the propagator $K(t-\tau) \propto 1/(t-\tau)^{1-\theta}$ must be replaced by $K(t-\tau) \propto 1/(t-\tau)^{1+\theta}$ for time difference larger than t^*. It would however be incorrect to deduce that we just have to change $-\theta$ into $+\theta$ in expressions (34) and (43), because the integrals leading to these results behave differently: as in (45), one has to re-introduced the regularization constant c to ensure convergence for $\tau \to t$ of $1/|t-\tau+c|^{1+\theta}$. The final results are thus given by (34) and (43) by changing $-\theta$ into $+\theta$ and by multiplying these expressions by the factor t^θ stemming from the regularization c. Thus, in the large time limit $t_c - t > t^*$ (far from the mainshock) of the subcritical regime, we also obtain an inverse Omori law which takes the form (28) for $a < \beta/2$ and the form (29) for $\beta/2 \leq a \leq \beta$. These predictions are in good agreement with our numerical simulations.

4. Prediction for the Gutenberg-Richter distribution of foreshocks

We have just shown that the stochastic component of the seismic rate can be formulated as a sum of the form (38) of variables x_i distributed according to a power law with exponent $m = \beta/a$ and weight K_i. It is possible to go beyond the derivation of the conditional expectation $\mathrm{E}[x_i|S_N]$ given by (39) and obtain the conditional distribution $p(x_i|S_N)$ conditioned on a large value of the realization of S_N.

For this, we use the definition of conditional probabilities

$$p(x_i|S_N) = \frac{p(S_N|x_i)p(x_i)}{P_N(S_N)} \ , \quad (46)$$

where $P_N(S_N)$ is the probability density function of the sum S_N. Since $p(S_N|x_i)$ is simply given by

$$p(S_N|x_i) = P_{N-1}(S_N - K_i x_i) \ , \quad (47)$$

we obtain

$$p(x_i|S_N) = p(x_i)\frac{P_{N-1}(S_N - K_i x_i)}{P_N(S_N)} \ . \quad (48)$$

This shows that the conditional Gutenberg-Richter distribution $p(x_i|S_N)$ is modified by the conditioning according to the multiplicative correcting factor $P_{N-1}(S_N - K_i x_i)/P_N(S_N)$. For large N, P_N and P_{N-1} tend to stable Lévy distributions with the same index m but different scale factors equal respectively to $\sum_j K_j^m$ and $\sum_{j \neq i} K_j^m$. The tail of $p(x_i|S_N)$ is thus

$$p(x_i|S_N) \sim \left(1 - \frac{K_i^m}{\sum_j K_j^m}\right) \frac{1}{x_i^{1+m}} \ \frac{1}{(1-(K_i x_i/S_N))^{1+m}} \ . \quad (49)$$

Since $K_i x_i \ll S_N$, we can expand the last term in the right-hand-side of (49) and obtain

$$p(x_i|S_N) \sim \left(1 - \frac{K_i^m}{\sum_j K_j^m}\right) \left[\frac{1}{x_i^{1+m}} + (1+m)(K_i/S_N)\frac{1}{x_i^m}\right] \ . \quad (50)$$

Since $x_i \sim E_i^a$, we use the transformation property of distribution functions $p(x_i)dX_i = p(E_i)dE_i$ to obtain the pdf of foreshock energies E_i. Going back to the continuous limit in which $K_i/S_N \sim (t_c-t)^{-(1-\theta)}/(t_c-t)^{-(1-\beta\theta)} = 1/(t_c-t)^{(\beta-1)\theta}$, we obtain the conditional Gutenberg-Richter distribution for foreshocks

$$P(E|\lambda_0) \sim \frac{E_0^\beta}{E^{1+\beta}} + \frac{C}{(t_c-t)^{\theta(\beta-a)/a}} \frac{E_0^{\beta'}}{E^{1+\beta'}} \qquad (51)$$

where

$$\beta' = \beta - a \ , \qquad (52)$$

and C is a numerical constant. The remarkable prediction (51) with (52) is that the Gutenberg-Richter distribution is modified upon the approach of a mainshock by developing a bump in its tail. This modification takes the form of an additive power law contribution with a new "b-value" renormalized/amplified by the exponent a quantifying the dependence of the number of daughters as a function of the energy of the mother. Our prediction is validated very clearly by numerical simulations reported in Figures 7 and 8.

5. Migration of foreshocks towards the mainshock

By the same mechanism leading to (34) via (30) and (32), conditioning the foreshock seismicity to culminate at a mainshock at time t_c at some point $\vec{r}$ taken as the origin of space must lead to a migration towards the mainshock. The seismic rate $\lambda(\vec{r},t)$ at position $\vec{r}$ at time $t < t_c$ conditioned on the existence of the mainshock at position $\vec{0}$ at time t_c is given by

$$\mathrm{E}[\lambda(\vec{r},t)|\lambda(\vec{0},t_c)] \sim \int_{-\infty}^{t} d\tau \int d\vec{\rho}\, K(\vec{r}-\vec{\rho},t-\tau)\, K(\vec{\rho},t_c-\tau) \ . \qquad (53)$$

$K(\vec{r}-\vec{\rho},t-\tau)$ is the dressed spatio-temporal propagator giving the seismic activity at position $\vec{r}$ and time t resulting from a triggering earthquake that occurred at position $\vec{\rho}$ at a time τ in the past. Its expression is given in [*Helmstetter and Sornette*, 2002b] in a variety of situations. Assuming that the probability distribution for an earthquake to trigger an aftershock at a distance r is of the form

$$\rho(r) \sim 1/(r+d)^{1+\mu} \ , \qquad (54)$$

Helmstetter and Sornette [2002b] have shown that the characteristic size of the aftershock area slowly diffuses according to $R \sim t^H$, where the time t is counted from the time of the mainshock. For simplicity, d is taken independent of the mainshock energy. H is the Hurst exponent characterizing the diffusion given by

$$H = \frac{\theta}{\mu} \quad \text{for} \quad \mu < 2 \ , \quad H = \frac{\theta}{2} \quad \text{for} \quad \mu > 2 \ . \qquad (55)$$

This diffusion is captured by the fact that $K(\vec{r}-\vec{\rho},t-\tau)$ depends on $\vec{r}-\vec{\rho}$ and $t-\tau$ essentially through the reduced variable $|\vec{r}-\vec{\rho}|/(t-\tau)^H$. Then, expression (53) predicts that this diffusion must be reflected into an inward migration of foreshock seismicity towards the mainshock with the same exponent H.

These results are verified by numerical simulations of the ETAS model. Figure 9 presents the migration of foreshock activity for two numerical simulations of the ETAS model, with different parameters. As for the inverse Omori law, we have superposed many sequences of foreshock activity to observe the migration of foreshocks. For a numerical simulation with parameters $n = 1$, $\theta = 0.2$, $\mu = 1$, $d = 1$ km, $c = 0.001$ day, $a = 0.5\beta$ and $m_0 = 2$, we see clearly the localization of the seismicity as the mainshock approaches. We obtain an effective migration exponent $H = 0.18$, describing how the effective size R of the cloud of foreshocks shrinks as time t approaches the time t_c of the main shock: $R \sim (t_c - t)^H$ (see Figure 9a,c). This result is in good agreement with the prediction $H = 0.2$ given by (55). The spatial distribution of foreshocks around the mainshock is similar to the distribution of aftershocks around the mainshock. Figure 9b,c presents the migration of foreshock activity for a numerical simulation with $\theta = 0.01$, $\mu = 1$, $d = 1$ km, $c = 0.001$ day leading to a very small diffusion exponent $H = 0.01$. The analysis of this foreshock sequence gives an effective migration exponent $H = 0.04$ for short times, and a faster apparent migration at longer times due to the influence of the background activity. See [*Helmstetter and Sornette*, 2002b] for a discussion of artifacts leading to apparent diffusions of seismicity resulting from various crossover phenomena.

6. Discussion

It has been proposed for decades that many large earthquakes were preceded by an unusually high seismicity rate, for times of the order of weeks to months before the mainshock [*Omori*, 1908; *Richter*, 1958; *Mogi*, 1963]. Although there are large fluctuations in the foreshock patterns from one sequence to another one, some recurrent properties are observed.

(i) The rate of foreshocks increases as $1/(t_c - t)^{p'}$ as a function of the time to the main shock at t_c, with an exponent p' smaller than or equal to the exponent p of direct Omori law;

(ii) the Gutenberg-Richter distribution of magnitudes is modified as the mainshock approaches, and is usually modeled by a decrease in b-value;

(iii) The epicenters of the foreshocks seem to migrate towards the mainshock.

We must acknowledge that the robustness of these three laws decreases from (i) to (iii). In previous sections, we have shown that these properties of foreshocks derive simply from the two most robust empirical laws of earthquake occurrence, namely the Gutenberg-Richter and Omori laws, which define the ETAS model. In this ETAS framework, foreshock sequences emerge on average by conditioning seismicity to lead to a burst of seismicity at the time of the mainshock. This analysis differs from two others analytical studies of the ETAS model [*Helmstetter and Sornette*, 2002b; *Sornette and Helmstetter*, 2002], who proposed that accelerating foreshock sequences may be related either to the super-critical regime $n > 1$ or to the singular regime $a > \beta$ (leading formally to $n \to \infty$) of the ETAS model. In these two regimes, an accelerating seismicity sequence arises from the cascade of aftershocks that trigger on average more than one aftershock per earthquake. Here we show that foreshock sequences emerge in the stationary sub-critical regime ($n < 1$) of the ETAS model, when an event triggers on average less than one aftershock. In this regime, aftershock have a low probability of triggering a larger earthquake. Nonetheless, conditioning on a high seismicity rate at the time of the mainshock, we observe, averaging over many mainshocks, an increase of the seismicity rate following the inverse Omori law. In addition, as we shall show below, this increase of seismicity has a genuine and significant predictive power.

6.1. Difference between type I and type II foreshocks

Our results applies to foreshocks of type II, defined as earthquakes preceding a mainshock in a space-time window preceding a mainshock, independently of their magnitude. This definition is different from the usual definition of foreshocks, which imposes a mainshock to be larger than the foreshocks (foreshocks of type I in our terminology). Using the usual definition of foreshocks in our numerical simulations of the ETAS model, our results remain robust but there are quantitative differences introduced by the somewhat arbitrary constraint entering into the definition of foreshocks of type I:

1. a roll-off in the inverse Omori-law,

2. a dependence of the apparent exponent p' on the time window used to define foreshocks and mainshocks and

3. a dependence of the rate of foreshocks and of p' on the mainshock magnitude.

As seen in Figure 5, these variations between foreshocks of type I and type II are observed only for small mainshocks. Such foreshocks are less likely the foreshocks of a mainshock and are more likely to be preceded by a larger earthquake, that is, to be the aftershocks of a large preceding mainshock. These subtle distinctions should attract the attention of the reader on the arbitrariness underlying the definition of foreshocks of type I and suggest, together with our results, that foreshocks of type II are more natural objects to define and study in real catalogs. This will be reported in a separate presentation.

6.2. Inverse Omori law

Conditioned on the fact that a mainshock is associated with a burst of seismicity, the inverse Omori law arises from the expected fluctuations of the seismicity rate leading to this burst of seismicity. Depending on the branching ratio n and on the ratio a/β, the exponent p' is found to vary between $1 - 2\theta$ and $1 + \theta$, but is always found to be smaller than the p exponent of the direct Omori law. Our results thus reproduce both the variability of p' and the lower value measured for p' than for p reported by [*Papazachos*, 1973, 1975b; *Page*, 1986; *Kagan and Knopoff*, 1978; *Jones and Molnar*, 1979; *Davis and Frohlich*, 1991; *Shaw*, 1993; *Utsu et al.*, 1995; *Ogata et al.*, 1995; *Maeda*, 1999]. In their synthesis of all p and p' values, *Utsu et al.* [1995] report p'-value in the range 0.7-1.3 , while p of aftershocks ranges from 0.9 to 1.5. The few studies that have measured simultaneously p and p' using a superposed epoch analysis have obtained p' either roughly equal to p [*Kagan and Knopoff*, 1978; *Shaw*, 1993] or smaller than p [*Davis and Frohlich*, 1991; *Ogata et al.*, 1995; *Maeda*, 1999]. The finding that $p \approx p' \approx 1$ suggested by [*Shaw*, 1993; *Reasenberg*, 1999] for the California seismicity can be interpreted in our framework as either due to a very small

θ value, or due to a large a/β ratio close to 0.8, as shown in Figures 4 and 6. The result $p' < p$ reported by [*Maeda*, 1999] for the Japanese seismicity and by *Davis and Frohlich* [1991] for the worldwide seismicity can be related to a rather small a/β ratio, as also illustrated in Figures 3 and 6.

In contrast with the direct Omori law, which is clearly observed after all large shallow earthquakes, the inverse Omori law is an average statistical law, which is observed only when stacking many foreshock sequences. Simulations reported in Figure 2 illustrate that, for individual foreshock sequences, the inverse Omori law is difficult to capture. Similarly to what was done for real data [*Kagan and Knopoff*, 1978; *Jones and Molnar*, 1979; *Davis and Frohlich*, 1991; *Shaw*, 1993; *Ogata et al.*, 1995; *Maeda*, 1999; *Reasenberg*, 1999], the inverse Omori law emerges clearly in our model only when using a superposed epoch analysis to average the seismicity rate over a large number of sequences. Our results are thus fundamentally different from the critical point theory [*Sammis and Sornette*, 2002] which leads to a power-law increase of seismic activity preceding each single large earthquake over what is probably a larger space-time domain [*Keilis-Borok and Malinovskaya*, 1964; *Bowman et al.*, 1998]. The inverse Omori law is indeed usually observed for time scales of the order of weeks to months before a mainshock, while *Keilis-Borok and Malinovskaya* [1964] and *Bowman et al* [1998] report a precursory increase of seismic activity for time scales of years to decades before large earthquakes. Our results can thus be considered as providing a null-hypothesis against which to test the critical point theory.

6.3. Foreshock occurrence rate

In term of occurrence rate, foreshocks are less frequent than aftershocks (e.g. [*Kagan and Knopoff*, 1976, 1978; *Jones and Molnar*, 1979]). The ratio of foreshock to aftershock numbers is close to 2-4 for $M = 5 - 7$ mainshocks, when selecting foreshocks and aftershocks at a distance $R = 50 - 500$ km from the mainshock and for a time $T = 10 - 100$ days before or after the mainshock [*Kagan and Knopoff* 1976; 1978; *Jones and Molnar*, 1979; *von Seggern et al.*, 1981; *Shaw*, 1993]. In our simulations, large mainshocks have significantly more aftershocks than foreshocks, in agreement with observations, while small earthquakes have roughly the same number of foreshocks (of type II) and of aftershocks. The ratio of aftershocks to foreshock of type II increases if the ratio a/β decreases, as observed when comparing the case $a = 0.5\beta$ shown in Figure 3 with the results obtained in the case $a = 0.8\beta$ represented in Figure 4. This may be explained by the relatively larger weights of the largest earthquakes which increase with increasing a, and by our definition of aftershocks and foreshocks: recall that aftershock sequences are conditioned on not being preceded by an event larger than the mainshock, whereas a foreshock of type II can be larger than the mainshock. Thus, for large $a/\beta < 1$, most "mainshocks", according to our definition, are aftershocks of a preceding large earthquake, whereas aftershock sequences cannot be preceded by an earthquake larger than the mainshock.

The retrospective foreshock frequency, that is, the fraction of mainshocks that are preceded by a foreshock, is reported to range from 10% to 40% using either regional or worldwide catalogs [*Jones and Molnar*, 1979; *von Seggern et al.*, 1981; *Yamashina*, 1981; *Console et al.*, 1983; *Jones*, 1984; *Agnew and Jones*, 1991; *Lindh and Lim*, 1995; *Abercrombie and Mori*, 1996; *Michael and Jones*, 1998; *Reasenberg*, 1999]. The variability of the foreshock rate is closely related to the catalog threshold for the magnitude completeness for the small events [*Reasenberg*, 1999]. These results are in line with our simulations.

The observed number of foreshocks per mainshock slowly increases with the mainshock magnitude [e.g. data from *Kagan and Knopoff*, 1978; *Shaw*, 1993; *Reasenberg*, 1999]. In our model, the number of foreshocks of type II is independent of the mainshock magnitude, because the magnitude of each earthquake is independent of the previous seismicity history. An increase of the number of foreshocks of type I as a function of the mainshock magnitude is observed in our numerical simulations (see Figure 5) because, as we explained before, the constraint on the foreshock magnitudes to be smaller than the mainshock magnitude is less severe for larger earthquakes and thus filter out less foreshocks. Therefore, our results can explain the increase in the foreshock frequency with the mainshock magnitude reported using foreshocks of type I. The slow increase of the number of foreshocks with the mainshock magnitude, if any, is different from the predictions of both the nucleation model [*Dodge et al.*, 1996] and of the critical point theory [*Sammis and Sornette*, 2002] which predict an increase of the foreshocks rate and of the foreshock zone with the mainshock size.

6.4. Magnitude distribution of foreshocks

Many studies have found that the apparent b-value of the magnitude distribution of foreshocks is smaller than that of the magnitude distribution of the background seismicity and of aftershocks. Case histories analyze individual foreshock sequences, most of them being chosen a posteriori to suggest that foreshock patterns observed in acoustic emissions preceding rupture in the laboratory could apply to earthquakes [*Mogi*, 1963; 1967]. A few statistical tests validate the significance of reported anomalies on b-value of foreshocks. A few others studies use a stacking method to average over many sequences in order to increase the number of events.

A b-value anomaly, usually a change in the mean b-value, for earthquakes preceding a mainshock has been proposed as a possible precursor on many retrospective case studies [*Suyehiro*, 1966; *Papazachos et al.*, 1967; *Ikegami*, 1967; *Berg*, 1968; *Bufe*, 1970; *Fedotov et al.*, 1972; *Wyss and Lee*, 1973; *Papazachos*, 1975a,b; *Ma*, 1978; *Li et al.*, 1978; *Wu et al.* 1978; *Cagnetti and Pasquale*, 1979; *Stephens et al.*, 1980; *Smith*, 1981, 1986; *Imoto* 1991; *Enescu and Kito*, 2001]. Most case histories argue for a decrease of b-value, but this decrease, if any, is sometimes preceded by an increase of b-value [*Ma*, 1978; *Smith*, 1981, 1986; *Imoto* 1991]. In a couple of cases, temporal decreases in b-value before Chinese earthquakes were used to issue successful predictions [*Wu et al.*, 1978; *Zhang et al.*, 1999].

Because of the paucity of the foreshock numbers, most of the study of individual sequences does not allow to estimate a robust temporal change of b-values before mainshocks, nor to characterize the shape of the magnitude distribution. A few studies have demonstrated the statistical significance of decreases of b-value when the time to the mainshock decreases using a superposed epoch analysis [*Kagan and Knopoff*, 1978; *Molchan and Dmitrieva, 1990*; *Molchan et al.*, 1999]. Using 200 foreshocks sequences of regional and worldwide seismicity, *Molchan et al.* [1999] found that the b-value is divided by a factor approximately equal to 2 a few days or hours before the mainshock. *Knopoff et al.* [1982] found no significant differences between the b-value of aftershocks and foreshocks when investigating 12 individual sequences of California catalogs. When all the aftershocks and foreshocks in a given catalog are superposed, the same study showed for catalogs of large durations (e.g. ISC, 1964-1977; NOAA, 1965-1977) that the b-value for foreshocks is significantly smaller than the b-value for aftershocks [*Knopoff et al.*, 1982]. The same pattern being simulated by a branching model for seismicity, *Knopoff et al.* [1982] surmise that the observed and simulated changes in magnitude distribution value arises intrinsically from the conditioning of aftershocks and foreshocks and from the smaller numbers of foreshocks relatively to aftershocks numbers when counted from the mainshock time. The result of [*Knopoff et al.*, 1982] is often cited as disproving the reality of a change of b-value. Our results find that a change in b-value in the ETAS branching model of seismicity is a physical phenomenon with real precursory content. This shall be stressed further below in association with Figure 10. Therefore, the fact that a change in b-value can be reproduced by a branching model of seismicity cannot discredit the strong empirical evidence of a change of b-value [*Knopoff et al.*, 1982] and its genuine physical content capturing the interactions between and triggering of earthquakes.

The observed modification of the magnitude distribution of foreshocks is usually interpreted as a decrease of b-value as the mainshock approaches. However, some studies argue that the Gutenberg-Richter distribution before a mainshock is no more a pure power-law distribution, due to an apparent increase of the number of large events relatively to the Gutenberg-Richter law, while the rate of small earthquakes remains constant. Such pattern is suggested by *Rotwain et al.* [1997] for both acoustic emission preceding material failure, and possibly for Californian seismicity preceding large earthquakes. Analysis of seismicity before recent large shocks also argue for an increase in the rate of moderate and large earthquakes before a mainshock [*Jaumé and Sykes*, 1999]. *Knopoff et al.* [1982] also suspected a deviation from a linear Gutenberg-Richter distribution for foreshocks. Our study of the ETAS model confirms that such a modification of the magnitude distribution before a mainshock must be expected when averaging over many foreshock sequences.

Intuitively, the modification of the magnitude distribution arises in our model from the increase of the aftershock rate with the mainshock magnitude. Any event has thus a higher probability to occur just after a large event, because this large event induces an increase of the seismicity rate. The novel properties that we demonstrate is that, before a mainshock, the energy distribution is no more a pure power-law, but it is the sum of the unconditional distribution with exponent β and an additional deviatoric power-law

distribution with a smaller exponent $\beta' = \beta - a$ as seen from expression (51). In addition, we predict and verify numerically in figures 7 and 8 that the amplitude of the deviatoric term increases as a power-law of the time to the mainshock. A similar behavior has been proposed as a precursory pattern termed "pattern upward bend" [*Keilis-Borok et al.*, 2001] or alternatively providing "pattern γ" measured as the difference between the slope of the Gutenberg-Richter for low and for large magnitudes. According to our results, pattern γ should increase from 0 to the value a.

According to the ETAS model, the modification of the magnitude distribution is independent of the mainshock magnitude, as observed by [*Kagan and Knopoff*, 1978; *Knopoff et al.* 1982; *Molchan and Dmitrieva*, 1990; *Molchan et al.*, 1999]. Therefore, all earthquakes, whatever their magnitude, are preceded on average by an increase of the rate of large events. Although the foreshock magnitude distribution is no more strictly speaking a pure power-law but rather the sum of two power laws, a single power-law distribution with a decreasing b-value as the time of the mainshock is approached is a simple and robust way to quantify the increasing importance of the tail of the distribution, especially for the short foreshock sequences usually available. This rationalizes the suggestion found in many works that a decrease in b-value is a (retrospective) signature of an impending mainshock. The novel insight provided by our analysis of the ETAS model is that a better characterization of the magnitude distribution before mainshocks may be provided by the sum of two power law distributions expressed by equation (51) and tested in synthetic catalogs in Figures 7 and 8. This rationalizes both the observed relatively small b-values reported for foreshocks and the apparent decrease of b-value when the mainshock approaches. Similarly to the inverse Omori law, the modification of the magnitude distribution prior the mainshock is a statistical property which yields an unambiguous signal only when stacking many foreshock sequences. This may explain the variability of the patterns of b-value observed for individual foreshock sequences.

A modification of the magnitude distribution before large earthquakes is also expected from the critical point theory [*Sammis and Sornette*, 2002]. The energy distribution far from a critical point is characterized by a power-law distribution with an exponential roll-off. As the seismicity evolves towards the critical point, the truncation of the energy distribution increases. At the critical point, the average energy becomes infinite (in an infinite system) and the energy distribution follows a pure power-law distribution. This modification of the seismicity predicted by the critical point theory is different from the one reported in this study, but the two models yield an apparent decrease of b-value with the time from the mainshock. Therefore, it is difficult to distinguish the two models in real seismicity data. However, the difference between the two models is that a modification of the energy distribution should only be observed before major earthquakes according to the critical point theory. Of course, one can not exclude that both mechanisms occur and are mixed up in reality.

6.5. Implications for earthquake prediction

The inverse Omori law and the apparent decrease of b-value have been derived in this study as statistical laws describing the average fluctuations of seismicity conditioned on leading to a burst of seismicity at the time of the mainshock. This does not mean that there is not a genuine physical content in these laws. We now demonstrate that they may actually embody an important part of the physics of earthquakes and describe the process of interactions between and triggering of earthquakes by other earthquakes. For this purpose, we use the modification of the magnitude frequency and the increase of the seismicity rate as predicting tools of future individual mainshocks. In the present work, we restrict our tests to the ETAS branching model used as a playing ground for our ideas.

Using numerical simulations of the ETAS model generated with $b = 1$, $a = 0.5\beta$, $n = 1$, $m_0 = 3$ and $\theta = 0.2$, we find that large earthquakes occur more frequently following a small locally estimated b-value. We have measured the b-value using a maximum likelihood method for a sliding window of 100 events. For instance, we find that 29% of the large $M > 6$ mainshocks occur in a 11% time period where β is less than 95% of the actual b-value (that is $b < 0.95$). This leads to a significant prediction gain of $g = 2.7$, defined as the ratio of the successful prediction (29%) over the duration of the alarms (11%) [*Aki*, 1981]. A random prediction would lead $g = 1$.

A much larger gain can be obtained using other precursory indicators related to the inverse Omori law. First, a large earthquake is likely to occur following another large earthquake. For the same simulation, fixing an alarm if the largest event within the 100 preceding earthquakes is larger that $M = 6$

yields a probability gain $g = 10$ for the prediction of a mainshock of magnitude equal to or larger than $M = 6$. Second, a large seismicity rate observed at a given "present" time will lead on average to a large seismicity rate in the future, and thus it increases the probability of having a large earthquake. Measuring the seismicity rate over a sliding window with flexible length imposed to contain exactly 100 events and fixing the alarm threshold at 0.05 events per day, we are able to predict 20% of the $M \geq 6$ events with just 0.16% of the time period covered by the alarms. This gives a prediction gain $g = 129$.

Figure 10 synthesizes and extends these results by showing the so-called error diagram [*Molchan*, 1991; 1997] for each of three functions measured in a sliding window of 100 events: (i) the maximum magnitude M_{max} of the 100 events in that window, (ii) the apparent Gutenberg-Richter exponent β measured on these 100 events by the standard Hill maximum likelihood estimator and (iii) the seismicity rate r defined as the inverse of the duration of the window containing 100 events. For each function, an alarm is declared for the next event when the function is either larger (for M_{max} and r) or smaller (for β) than a threshold. Scanning all possible thresholds constructs the continuous curves shown in the figure. The results on the prediction obtained by using these three precursory functions are considerably better than those obtained for a random prediction, shown as a dashed line for reference. We have not tried at all to optimize any facet of these prediction tests, which are offered for the sole purpose of stressing the physical reality of the precursory information contained in the foreshocks.

6.6. Migration of foreshocks

Among the proposed patterns of foreshocks, the migration of foreshocks towards the mainshocks is much more difficult to observe than either the inverse Omori law or the change in b-value. This is due to the limited number of foreshocks and to the location errors. Similarly to other foreshock patterns, a few case-histories have shown seismicity migration before a mainshock. When reviewing 9 $M > 7$ shallow earthquakes in China, *Ma et al.* [1990] report a migration of $M > 3 - 4$ earthquakes towards the mainshock over a few years before the mainshock and at a distance of a few hundreds of kilometers. Less than 20 events are used for each case study. While the case for the diffusion of aftershocks is relatively strong [*Kagan and Knopoff*, 1976, 1978; *von Seggern et al.*, 1981; *Tajima and Kanamori*, 1985] but still controversial, the migration of foreshocks towards the mainshock area, suggested using a stacking method [e.g., *Kagan and Knopoff*, 1976, 1978; *von Seggern et al.*, 1981; *Reasenberg*, 1985] is even less clearly observed.

Using the ETAS model, *Helmstetter and Sornette* [2002b] have shown that the cluster of aftershocks diffuses on average from the mainshock according to the diffusion law $R \sim t^H$, where R is the typical size of the cluster and H is the so-called Hurst exponent which can be smaller or larger than 1/2. In the present study, we have shown analytically and numerically that this diffusion of aftershocks must be reflected into a (reverse) migration of seismicity towards the mainshock, with the same diffusion exponent H (defined in (55)). We should however point out that this predicted migration of foreshocks, as well as the diffusion of aftershocks, is significant only over a finite domain of the parameter space over which the ETAS model is defined. Specifically, a significant spatio-temporal coupling of the seismicity leading to diffusion and migration is expected and observed in our simulations only for sufficiently large θ's and for short times $|t_c - t| < t^*$ from the mainshock, associated with a direct Omori exponent p smaller than 1. This may explain why the diffusion of aftershocks and the migration of foreshocks is often difficult to observe in real data.

An additional difficulty in real data arises from the background seismicity, which can induce a spurious diffusion of aftershocks or migration of foreshocks (see Figure 9c). As for the other foreshock patterns derived in this study, the migration of foreshocks towards the mainshock and the spatial distribution of foreshocks are independent of the mainshock magnitude. These results disagree with the observations of [*Keilis-Borok and Malinovskaya*, 1964; *Bowman et al.*, 1998] who suggest that the area of accelerating seismicity prior a mainshock increases with the mainshock size. An increase of the foreshock zone with the mainshock size may however be observed in the ETAS model when using foreshocks of type I (conditioned on being smaller than the mainshock) and introducing a characteristic size of the aftershock zone d in (54) increasing with the mainshock size.

7. Conclusion

We have shown that the ETAS (epidemic-type aftershock) branching model of seismicity, based on the two best established empirical Omori and Gutenberg-Richter laws, contains essentially all the phenomenol-

ogy of foreshocks. Using this model, decades of empirical studies on foreshocks are rationalized, including the inverse Omori law, the b-value change and seismicity migration. For each case, we have derived analytical solutions that relates the foreshock distributions in the time, space and energy domain to the properties of a simple earthquake triggering process embodied by aftershocks. We find that all previously reported properties of foreshocks arises from the Omori and Gutenberg-Richter law when conditioning the spontaneous fluctuations of the rate of seismicity to end with a burst of activity, which defines the time of the mainshock. The foreshocks laws are seen as statistical laws which are clearly observable when averaging over a large number of sequences and should not be observed systematically when looking at individual foreshock sequences. Nevertheless, we have found that foreshocks contain genuine important physical information of the triggering process and may be used successfully to predict earthquakes with very significant probability gains. Taking these results all together, this suggests that the physics of aftershocks is sufficient to explain the properties of foreshocks, and that there is no essential physical difference between foreshocks, aftershocks and mainshocks.

Acknowledgments. We are very grateful to Y.Y. Kagan, G. Ouillon and V. Pisarenko for useful suggestions and discussions, and for R. Schoenberg for a constructive review of the manuscript. This work was partially supported by french INSU-Natural Hazard grant (AH and JRG) and by the James S. Mc Donnell Foundation 21st century scientist award/studying complex system (DS).

Appendix A: Deviations from the average seismicity rate

Using the definition of $\lambda(t)$ (8), in the case where the external $s(t)$ source term is a Dirac $\delta(t)$, we obtain the following expression for the stochastic propagator

$$\kappa(t) = \delta(t) + \int_{-\infty}^{t} d\tau \int_{E_0}^{+\infty} dE\ \phi_E(t-\tau) \sum_{i\ |\ t_i \le t} \delta(E-E_i)\,\delta(\tau - t_i)\ , \tag{A1}$$

We now express the deviation of $\kappa(t)$ from its ensemble average $K(t)$. This can be done by using (12), which means that the distribution density of earthquake energies is constructed by recording all earthquakes and by counting the frequency of their energies. Thus, $\delta(E-E_\tau)$ can be seen as the sum of its average plus a fluctuation part, namely, it can be formally expressed as $\delta(E-E_\tau) = P(E) + \delta P(E)$, where $\delta P(E)$ denotes the fluctuation of $\delta(E-E_\tau)$ around its ensemble average $P(E)$. Similarly, $\kappa(t) = \sum_{t_i \le t} \delta(t-t_i) = K(t) + \delta\kappa(t)$, where $\delta\kappa(t)$ is the fluctuating part of the seismic rate around its ensemble average $K(t)$.

We can thus express the sum of products of Dirac functions in (A1) as follows:

$$\sum_{i\ |\ t_i \le t} \delta(E-E_i)\delta(t-t_i) = P(E)K(t) + \delta(P\kappa)(E,t)\ . \tag{A2}$$

As a first illustration, we can use the approximation that the fluctuations of the product $\delta(E-E_\tau)\sum_{t_i\le t}\delta(t-t_i)$ can be factorized to write

$$\delta(E-E_t)\sum_{t_i\le t}\delta(t-t_i) = \left(P(E)+\delta P(E)\right)\left(K(t)+\delta\kappa(t)\right)$$

$$\approx P(E)K(t) + P(E)\ \delta\kappa(t) + K(t)\ \delta P(E)\ . \tag{A3}$$

Using expression (A1) for $\kappa(t)$ and expression (15) for $K(t)$, and putting (A3) in (A1), we then obtain

$$\kappa(t) = K(t) + \int_0^t d\tau \int_{E_0}^{+\infty} dE\ \phi_E(t-\tau)\delta(P\kappa)(E,\tau)\ , \tag{A4}$$

where

$$\delta(P\kappa)(E,\tau) \equiv \delta P(E)K(\tau) + P(E)\delta\kappa(t)\ . \tag{A5}$$

By construction, the average of the double integral in the r.h.s. of (A4) is zero. The double integral thus represents the fluctuating part of the realization specific seismic response $\kappa(t)$ to a triggering event. Inserting (A4) in (22), we obtain

$$\lambda(t) = N(t) +$$
$$\int_{-\infty}^{t} d\tau\ s(\tau) \int_0^{t-\tau} du \int_{E_0}^{+\infty} dE\ \phi_E(t-\tau-u)\delta(P\kappa)(E,u)\ . \tag{A6}$$

Using $\int_{-\infty}^{t} d\tau \int_0^{t-\tau} du = \int_0^{+\infty} du \int_{-\infty}^{t-u} d\tau$, expression (A6) reads

$$\lambda(t) = N(t) +$$
$$\int_{E_0}^{+\infty} dE \int_0^{+\infty} du\ \delta(P\kappa)(E,u) \int_{-\infty}^{t-u} d\tau\ s(\tau)\ \phi_E(t-\tau-u)\ . \tag{A7}$$

For instance, let us consider the first contribution $\delta P(E)K(\tau)$ of $\delta(P\kappa)(E,\tau)$ given by (A5). Denoting

$$\epsilon \equiv \int_{E_0}^{+\infty} dE\ \rho(E)\ \delta P(E)\ , \tag{A8}$$

$\lambda(t)$ given by (A7) is of the form (23) with

$$\eta(\tau) = \epsilon \int_0^{+\infty} dx\ s(\tau - x)\ \Psi(x)\ , \tag{A9}$$

where $\Psi(x)$ is the bare Omori propagator defined in (4).

The only property needed below is that the stochastic process $\eta(\tau)$ be stationary. This is the case because the fluctuations of $\delta P(E)$ and of the source $s(t)$ are stationary processes. Similarly, the second contribution $P(E)\delta\kappa(\tau)$ of $\delta(P\kappa)(E,\tau)$ given by (A5) takes the form (23) if $\delta\kappa(\tau)$ is a noise proportional to $K(t)$. At present, we cannot prove it but this seems a natural assumption. More generally, one could avoid the decomposition of $\delta(P\kappa)(E,\tau)$ given by (A5) and get the same result as long as $\delta(P\kappa)(E,t)$ is equal to a stationary noise multiplying $K(t)$.

Appendix B: Conditioning weighted power law variables on the realization of their sum

Consider i.i.d. (identically independently distributed) random variables x_i distributed according to a power law $p(x_i)$ with exponent $m \leq 2$. Let us define the sum

$$S_N = \sum_{i=1}^{N} K_i x_i \ , \tag{B1}$$

where the K_i's are arbitrary positive weights. Here, we derive that the expectation $\mathrm{E}[x_i|S_N]$ of x_i conditioned on the existence of a large realization of S_N is given by (39).

By definition, $\mathrm{E}[x_i|S_N] = N/D$ where

$$N = \int dx_1 \, ... \int dx_N \, x_i \, p(x_1)...p(x_N) \, \delta \left(S_N - \sum_{j=1}^{N} K_j x_j \right) \ , \tag{B2}$$

and D is the same expression without the factor x_i. The Fourier transform of (B2) with respect to S_N yields

$$\hat{N}(k) = \left[\prod_{j \neq i} \hat{p}(kK_j) \right] \ \frac{1}{ik} \ \frac{d\hat{p}(kK_i)}{dK_i} = \frac{1}{ik} \ \frac{d}{dK_i} \left[\prod_{j=1} \hat{p}(kK_j) \right] \ . \tag{B3}$$

We have used the identity $\int dx_i \ x_i \ p(x_i) \ e^{ikK_i x_i} = \frac{1}{ik} \ \frac{d\hat{p}(kK_i)}{dK_i}$ and $\hat{p}(k)$ is the Fourier transform of $p(x)$. Note that $\prod_{j=1}^{N} \hat{p}(kK_j)$ is nothing but the Fourier transform $\hat{P}_S(k)$ of the distribution $P_N(S_N)$. Using the elementary identities of derivatives of Fourier transforms and by taking the inverse Fourier transform, we thus get

$$N = \frac{d}{dK_i} \int_{S_N}^{+\infty} dX \ P_N(X) \ . \tag{B4}$$

By definition, the denominator D is identically equal to $P_N(S_N)$. This yields the general result

$$\mathrm{E}[x_i|S_N] = \frac{1}{P_N(S_N)} \ \frac{d}{dK_i} \int_{S_N}^{+\infty} dX \ P_N(X) \ . \tag{B5}$$

In the special case where all K_i's are equal, this gives the "democratic" result $\mathrm{E}[x_i|S_N] = S_N/N$.

For power law variables with distribution $p(x) \sim 1/x^{1+m}$ with $m < 2$, we can use the generalized central limit theorem to obtain that $P_N(X)$ converges for large N to a stable Lévy law L_m with index equal to the exponent m and scale factor $\sum_{j=1}^{N} K_j^m$ [*Gnedenko and Kolmogorov*, 1954; *Sornette*, 2000]:

$$P_N(S_N) \rightarrow_{N \rightarrow \infty} L_m \left(\frac{S_N}{\left(\sum_{j=1}^{N} K_j^m \right)^{1/m}} \right) \ . \tag{B6}$$

The only dependence of $P_N(S_N)$ in K_i is found in the scale factor. Putting the expression (B6) into (B5) yields the announced result (39). In particular, for $m = 2$, this recovers the standard result for Gaussian variables that $\mathrm{E}[x_i|S_N] \sim S_N K_i$, because the stable Lévy law of index $m = 2$ is the Gaussian distribution.

References

Abercrombie, R. E., and J. Mori, Occurrence patterns of foreshocks to large earthquakes in the western United States, *Nature, 381*, 303-307, 1996.

Agnew, D. C. and L. M. Jones, Prediction probabilities from foreshocks, *J. Geophys. Res., 96*, 11,959-11971, 1991.

Aki, K., A probabilistic synthesis of precursory phenomena, in *Earthquake Prediction*, edited by D. W. Simpson and P. G. Richards, AGU Maurice Ewing series: 4, Washington, D.C., pp 556-574, 1981.

Berg, E., Relation between earthquake foreshocks, stress and mainshocks, *Nature, 219*, 1141-1143, 1968.

Bowman, D. D., G. Ouillon, C. G. Sammis, A. Sornette and D. Sornette, An observational test of the critical earthquake concept, *J. Geophys. Res., 103*, 24359-24372, 1998).

Bufe, C. G., Frequency magnitude variations during the 1970 Danville earthquake swarm, *Earthquake Notes, 41*, 3-7, 1970.

Cagnetti, V. and V. Pasquale, The earthquake sequence in Frieli, Italy, 1976, *Bull. Seism. Soc. Am., 69*, 1797-1818, 1979

Console, R., M. Murru and B. Alessandrini, Foreshocks statistics and their possible relationship to earthquake prediction in the Italian region, *Bull. Seism. Soc. Am., 83*, 1248-1263, 1983.

Daley, D. J. and D. Vere-Jones, *An Introduction to the theory of point processes*, Springer, 1988.

Davis, S. D. and C. Frohlich, Single-link cluster analysis of earthquake aftershocks: decay laws and regional variations, *J. Geophys. Res., 96*, 6335-6350, 1991.

Dodge, D. D., G. C. Beroza and W.L. Ellsworth, Detailed observations of California foreshock sequence: Implications for the earthquake initiation process, *J. Geophys.*

Res., 101, 22,371-22,392, 1996.

Enescu, B. and K. Ito, Some premonitory phenomena of the 1995 Hyogo-Ken Nanbu (Kobe) earthquake: seismicity, *b*-value and fractal dimension, *Tectonophysics*, *338*, 297-314, 2001.

Fedotov S. A., A. A. Gusev and S. A. Boldyrev, Progress in earthquake prediction in Kamchatka, *Tectonophysics*, *14*, 279-286, 1972.

Felzer, K. R., T. W. Becker, R. E. Abercrombie, G. Ekström and J. R. Rice, Triggering of the 1999 M_W 7.1 Hector Mine earthquake by aftershocks of the 1992 M_W 7.3 Landers earthquake, *J. Geophys. Res.*, 107, 2190, doi:10.1029/2001JB000911, 2002.

Gabrielov, A., I. Zaliapin, W. I. Newman and V. I. Keilis-Borok, Colliding cascades model for earthquake prediction, *Geophys. J. Int.,143*, 427-437, 2000a.

Gabrielov, A., V. Keilis-Borok, I. Zaliapin and W. I. Newman, Critical transitions in colliding cascades, *Phys. Rev. E*, *62*, 237-249, 2000b.

Gnedenko, B. V. and A. N. Kolmogorov, *Limit Distributions for Sum of Independent Random Variables*, Addison Wesley, Reading MA, 1954.

Gross, S. and C. Kisslinger, Tests of models of aftershocks rate decay, *Bull. Seism. Soc. Am.*, *84*, 1571-1579, 1994.

Guo, Z. and Y. Ogata, Statistical relations between the parameters of aftershocks in time, space and magnitude, *J. Geophys. Res.*, *102*, 2857-2873, 1997.

Hainzl, S., G. Zoller and J. Kurths, Similar power laws for foreshock and aftershock sequences in a spring-block model for earthquakes, *J. Geophys. Res., 104*, 7243-7253, 1999.

Harris, T.E., *The theory of branching processes*, Springer, Berlin, 1963.

Helmstetter, A., Is earthquake triggering driven by small earthquakes?, *Phys. Res. Lett.*, 91, 058501, 2003

Helmstetter, A. and D. Sornette, Sub-critical and supercritical regimes in epidemic models of Earthquake Aftershocks, *J. Geophys. Res.*, 107, 2237, doi:10.1029/2001JB001580, 2002a.

Helmstetter, A. and D. Sornette, Diffusion of earthquake aftershock epicenters and Omori law: exact mapping to generalized continuous-time random walk models, *Phys. Rev. E*, 6606, 1104, doi:10.1103/PhysRevE.66.061104, 2002b.

Huang, Y., H. Saleur, C. Sammis and D. Sornette, Precursors, aftershocks, criticality and self-organized criticality, *Europhys. Lett., 41*, 43-48, 1998.

Ikegami, R, *Bull. Earth. Res. Inst., 45*, 328-345, 1967.

Imoto, M., Changes in the magnitude frequency *b*-value prior to large (M$\geq$ 6.0) earthquakes in Japan, *Tectonophysics*, *193*, 311-325, 1991.

Jacod, J. and A. N. Shiryaev, *Limit Theorems for Stochastic Processes*, Springer, Berlin, 1987.

Jaumé, S. C. and L. R. Sykes, Evolving towards a critical point: A review of accelerating seismic moment/energy release prior to large and great earthquakes, *Pure Appl. Geophys., 155*, 279-306, 1999.

Jones, L. M., Foreshocks (1966-1980) in the San Andreas system, California, *Bull. Seis. Soc. Am., 74*, 1361-1380, 1984.

Jones, L. M., and P. Molnar, Some characteristics of foreshocks and their possible relationship to earthquake prediction and premonitory slip on fault, *J. Geophys. Res.*, *84*, 3596-3608, 1979.

Jones, L. M., R. Console, F. Di Luccio and M. Murru, Are foreshocks mainshocks whose aftershocks happen to be big? preprint 1999 available at http://pasadena.wr.usgs.gov/office/jones/italy-bssa.html

Kagan, Y. Y., Aftershock zone scaling, *Bull. Seism. Soc. Am.*, *92*, 641-655, 2002.

Kagan, Y. Y. and L. Knopoff, Statistical search for nonrandom features of the seismicity of strong earthquakes, *Phys. Earth Planet. Int.*, *12*, 291-318, 1976.

Kagan, Y. Y. and L. Knopoff, Statistical study of the occurrence of shallow earthquakes, *Geophys. J. R. Astr. Soc.*, *55*, 67-86, 1978.

Kagan, Y. Y. and L. Knopoff, Stochastic synthesis of earthquake catalogs, *J. Geophys. Res.*, *86*, 2853-2862, 1981.

Kagan, Y. Y. and L. Knopoff, Statistical short-term earthquake prediction, *Science*, *236*, 1563-1467, 1987.

Keilis-Borok, V. I. and L. N. Malinovskaya, One regularity in the occurrence of strong earthquakes, *J. Geophys. Res.*, *69*, 3019-3024, 1964.

Keilis-Borok, V. and V. G. Kossobokov, Premonitory activation of earthquake flow - Algorithm M8, *Phys. Earth Planet. Int.*, *61*, 73-83, 1990.

Keilis-Borok, V., A. Ismail-Zadeh, V. Kossobokov and P. Shebalin, Non-linear dynamics of the lithosphere and intermediate-term earthquake prediction, *Tectonophysics*, *338*, 247-260, 2001.

Kisslinger, C., The stretched exponential function as an alternative model for aftershock decay rate, *J. Geophys. Res.*, *98*, 1913-1921, 1993.

Kisslinger, C. and L. M. Jones, Properties of aftershocks sequences in Southern California, *J. Geophys. Res.*, *96*, 11947-11958, 1991.

Knopoff, L., Y. Y. Kagan and R. Knopoff, *b*-values for fore- and aftershocks in real and simulated earthquakes sequences, *Bull. Seism. Soc. Am.*, *72*, 1663-1676, 1982.

Li, Q. L., J. B. Chen, L. Yu, and B. L. Hao, Time and space scanning of the *b*-value: A method for monitoring the development of catastrophic earthquakes, *Acta Geophys. Sinica, 21*, 101-125, 1978.

Lindh, A. G., and M. R. Lim, A clarification, correction and updating of Parkfield California, earthquakes prediction scenarios and response plans, *U.S. Geol. Surv. Open File Rep.*, 95-695, 1995.

Ma, H., Variation of the *b*-values before several large earthquakes that occurred in North China, *Acta Geophysica Sinica., 21*, 126-141, 1978, (in chinese).

Ma, Z., Fu Z., Zhang Y., Wang C., Zhang G. and D. Liu, *Earthquake prediction, nine major cas in China*, Seismological Press Beijing, Springer Verlag, 332 pp, 1990.

Maeda, K., Time distribution of immediate foreshocks obtained by a stacking method, *Pure Appl. Geophys., 155*, 381-384, 1999.

Michael, A. J. and L. M. Jones, Seismicity alert probabilities at Parkfield, California, revisited, *Bull. Seis. Soc. Am., 88*, 117-130, 1998.

Mogi, K. Some discussions on aftershocks, foreshocks and earthquake swarms, *Bull. Res. Inst., Tokyo, Univ., 41*, 595-614, 1963.

Mogi, K. Earthquakes and fractures, *Tectonophysics*, *5*, 35-55, 1967.

Molchan, G. M., Structure of optimal strategies in earthquake prediction, *Tectonophysics*, *193*, 267-276, 1991.

Molchan, G. M., Earthquake prediction as a decision-making problem, *Pure Appl. Geophys.*, *149*, 233-247, 1997.

Molchan, G. M. and O. Dmitrieva, Dynamics of the magnitude frequency relation for foreshocks *Phys. Earth. Plan. Inter.*, *61*, 99-112, 1990.

Molchan, G. M., T.L. Konrod and A.K. Nekrasova, Immediate foreshocks: time variation of the *b*-value, *Phys. Earth. Plan. Inter.*, *111*, 229-240, 1999.

Morse, P. M. and H. Feshbach, *Methods in Theoretical Physics*, McGraw-Hill, New-York, 1953.

Narteau, C., P. Shebalin, M., Holschneider, J. L. Le Mouel and C. Allègre, Direct simulations of the stress redistribution in the scaling organization of fracture tectonics (SOFT) model, *Geophys. J. Int.*, *141*, 115-135, 2000.

Ogata, Y., Statistical models for earthquake occurrence and residual analysis for point processes, *J. Am. stat. Assoc.*, *83*, 9-27, 1988.

Ogata, Y., T. Utsu and K. Katsura, Statistical features of foreshocks in comparison with others earthquakes clusters, *Geophys. J. Int., 121*, 233-254, 1995.

Ogata, Y., T. Utsu and K. Katsura, Statistical discrimination of foreshocks from other earthquakes clusters, *Geophys. J. Int., 127*, 17-30, 1996.

Omori, F., On the aftershocks of earthquakes, *J. Coll. Sci. Imp. Univ. Tokyo*, *7*, 111-120, 1894.

Omori, F., On Foreshocks of earthquakes, *Pub. Imp. Eartq. Inv. Com.*, *2*, 89-100, 1908.

Page, R.A., Comments on "earthquake frequency and prediction" by Liu Z.R., *Bull. Seis. Soc. Am.*, *74*, 1491-1496, 1986.

Papazachos, B. C., The time distribution of reservoir-associated foreshocks and its importance to the prediction of the principal shock, *Bull. Seis. Soc. Am., 63*, 1973-1978, 1973.

Papazachos, B. C., On certain aftershock and foreshock parameters in the area of Greece, *Ann., Geofis., 28*, 497-515, 1975a.

Papazachos, B., Foreshocks and earthquakes prediction, *Tectonophysics, 28*, 213-216, 1975b.

Papazachos, B., M. Delibasis, N. Liapis, G. Moumoulis and G. Purcaru, Aftershock sequences of some large earthquakes in the region of Greece, *Ann. Geofis., 20*, 1-93, 1967.

Pelletier, J. D., Spring-block models of seismicity/ Review and analysis of a structurally heterogeneous model coupled to a viscous asthenosphere, in *Geocomplexity and the physics of earthquakes*, edited by J.B. Rundle, D. L. Turcotte, and W. Klein, AGU, geophysical monograph 120, Washington D.C., 27-42, 2000.

Reasenberg P., Second order moment of central California seismicity, 1969-1982, *J. Geophys. Res., 90*, 5479-5495, 1985.

Reasenberg, P. A., Foreshocks occurrence before large earthquakes, *J. Geophys. Res.*, *104*, 4755-4768, 1999.

Reasenberg, P. A. and L. M. Jones, earthquake hazard after a mainshock in California, *Science*, *243*, 1173-1176, 1989.

Richter, C. F., *Elementary seismology*, 758 pp., W.H. Freeman and Co, San Francisco, 1968.

Rotwain, I., V. Keilis-Borok and L. Botvina, Premonitory transformation of steel fracturing and seismicity, *Phys. Earth Planet. Int.*, *101*, 61-71, 1997.

Sammis, S. G. and D. Sornette, Positive feedback, memory and the predictability of earthquakes, *Proceedings of the National Academy of Sciences*, *99*, 2501-2508, 2002.

Scholz, C. H., Microfractures, aftershocks, and seismicity, *Seism. Soc. of Am. Bull.*, *58*, 1117-1130, 1968.

von Seggern, D., S. S. Alexander and C-B Baag, Seismicity parameters preceding moderate to major earthquakes *J. Geophys. Res., 86*, 9325-9351, 1981.

Shaw, B. E., Generalized Omori law for aftershocks and foreshocks from a simple dynamics, *Geophys. Res. Letts.,10*, 907-910, 1993.

Smith, W.D., The *b*-value as an earthquake precursor, *Nature, 289*, 131-139,1981.

Smith, W.D., Evidence for precursory changes in the frequency-magnitude *b*-value, *Geophys., J. Roy. Astr. Soc., 86*, 815-838, 1986.

Sornette, A. and D. Sornette, Renormalization of earthquake aftershocks, *Geophys. Res. Lett.*, *26*, 1981-1984, 1999.

Sornette, D., *Critical Phenomena in Natural Sciences, Chaos, Fractals, Self-organization and Disorder: Concepts and Tools*, Springer Series in Synergetics, Heidelberg, 2000.

Sornette D. and A. Helmstetter, On the occurrence of finite-time-singularities in epidemic models of rupture, earthquakes and starquakes, *Phys. Rev. Lett., 89*, 158501, 2002 (http://arXiv.org/abs/cond-mat/0112043).

Sornette, D. and C.G. Sammis, Complex critical exponents from renormalization group theory of earthquakes : Implications for earthquake predictions, *J. Phys. I France*, *5*, 607-619, 1995.

Sornette, D., C. Vanneste and L. Knopoff, Statistical model of earthquake foreshocks, *Phys. Rev. A*, *45*, 8351-8357, 1992.

Stephens, C. D., J. C. Lahr, K. A. Fogleman and R.B. Horner, The St-Helias, Alaska, earthquake of february 28, 1979: regional recording of aftershocks and short-term, pre-earthquake seismicity, *Bull. Seis. Soc. Am., 70*, 1607-1633, 1980.

Suyehiro, S., Difference between aftershocks and foreshocks in the relationship of magnitude frequency of occurrence for the great chilean earthquake of 1960, *Bull. Seis. Soc. Am., 56*, 185-200, 1966.

Tajima, F. and H. Kanamori, Global survey of aftershock area expansion patterns, *Phys. Earth Planet. Inter., 40*, 77-134, 1985.

Utsu, T., Y. Ogata and S. Matsu'ura, The centenary of the Omori Formula for a decay law of aftershock activity, *J. Phys. Earth*, *43*, 1-33, 1995.

Wu, K.T., Yue, M.S., Wu, H.Y., Chao, S.L., Chen, H.T., Huang, W.Q., Tien, K.Y and S.D. Lu, Certain characteristics of the Haicheng earthquake (M=7.3) sequence, *Chinese Geophysics, AGU, 1*, 289-308, 1978.

Wyss, M. and W. H. K. Lee, Time variations of the average magnitude in central California, *Proceedings of the conference on Tectonic Problems of the San Andreas Fault System*, edited by R. Kocach and A. Nur, Stanford University Geol. Sci., 13, 24-42, 1973.

Yamanaka, Y. and K. Shimazaki, Scaling relationship between the number of aftershocks and the size of the mainshock, *J. Phys. Earth, 38*, 305-324, 1990.

Yamashina, K., Some empirical rules on foreshocks and earthquake prediction, in *Earthquake Prediction*, edited by D. W. Simpson and P. G. Richards, AGU Maurice Ewing series: 4, Washington, D.C., pp 517-526, 1981.

Yamashita, T. and L. Knopoff, Models of aftershock occurrence, *Geophys. J. R. Astron. Soc.*, *91*, 13-26, 1987.

Yamashita, T. and L. Knopoff, A model of foreshock occurrence. *Geophys. Journal*, *96*, 389-399, 1989.

Yamashita, T. and L. Knopoff, Model for intermediate-term precursory clustering of earthquakes, *J. Geophys. Res.*, *97*, 19873-19879, 1992.

Zhang G., Zhu L., Song, X., Li, Z., Yang, M., SU, N., X. Chen, Predictions of the 1997 strong earthquakes in Jiashi, Xinjiang, China, *Bull. Seis. Soc. Am., 89*, 1171-1183, 1999.

Zoller, G. and S. Hainzl, A systematic spatio-temporal test of the critical point hypothesis for large earthquakes, *Geophys. Res. Lett.*, accepted, 2002.

Agnès Helmstetter, Laboratoire de Géophysique Interne et Tectonophysique, Observatoire de Grenoble, Université Joseph Fourier, BP 53X, 38041 Grenoble Cedex, France. (e-mail: ahelmste@obs.ujf-grenoble.fr)

Didier Sornette, Department of Earth and Space Sciences and Institute of Geophysics and Planetary Physics, University of California, Los Angeles, California and Laboratoire de Physique de la Matière Condensée, CNRS UMR 6622 Université de Nice-Sophia Antipolis, Parc Valrose, 06108 Nice, France (e-mail: sornette@ess.ucla.edu)

Jean-Robert Grasso, Laboratoire de Géophysique Interne et Tectonophysique, Observatoire de Grenoble, Université Joseph Fourier, BP 53X, 38041 Grenoble Cedex, France. (e-mail:Jean-Robert.Grasso@obs.ujf-grenoble.fr)

This preprint was prepared with AGU's LaTeX macros v4. File InvOmoriRevised formatted May 16, 2006.

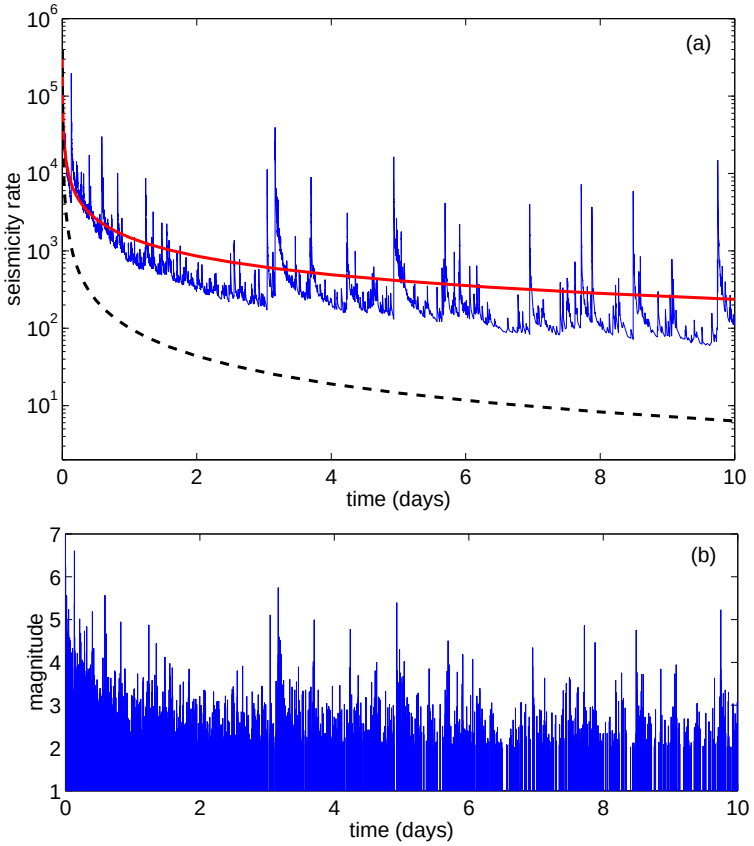

Figure 1. An example of a realization of the ETAS model, which illustrates the differences between the observed seismicity rate $\kappa(t)$ (noisy solid line), the average renormalized (or dressed) propagator $K(t)$ (solid line), and the local propagator $\phi_E(t)$ (dashed line). The magnitude of each earthquake are shown in panel (b). This aftershock sequence has been generated using the ETAS model with parameters $n = 1$, $a = 0.8\beta$, $\theta = 0.2$, $m_0 = 2$ and $c = 0.001$ day, starting from a mainshock of magnitude $M = 7$ at time $t = 0$. The global aftershock rate $\kappa(t)$ is significantly higher than the direct (or first generation) aftershock rate, described by the local propagator $\phi_E(t)$. The global aftershock rate $\kappa(t)$ decreases on average according to the dressed propagator $K(t) \sim 1/t^{1-\theta}$, which is significantly slower than the local propagator $\phi(t) \sim 1/t^{1+\theta}$. The best fit to the observed seismicity rate $\kappa(t)$ is indistinguishable from the average dressed propagator $K(t)$. Large fluctuations of the seismicity rate corresponds to the occurrence of large aftershocks, which trigger their own aftershock sequence. Third-generation aftershocks can be easily observed.

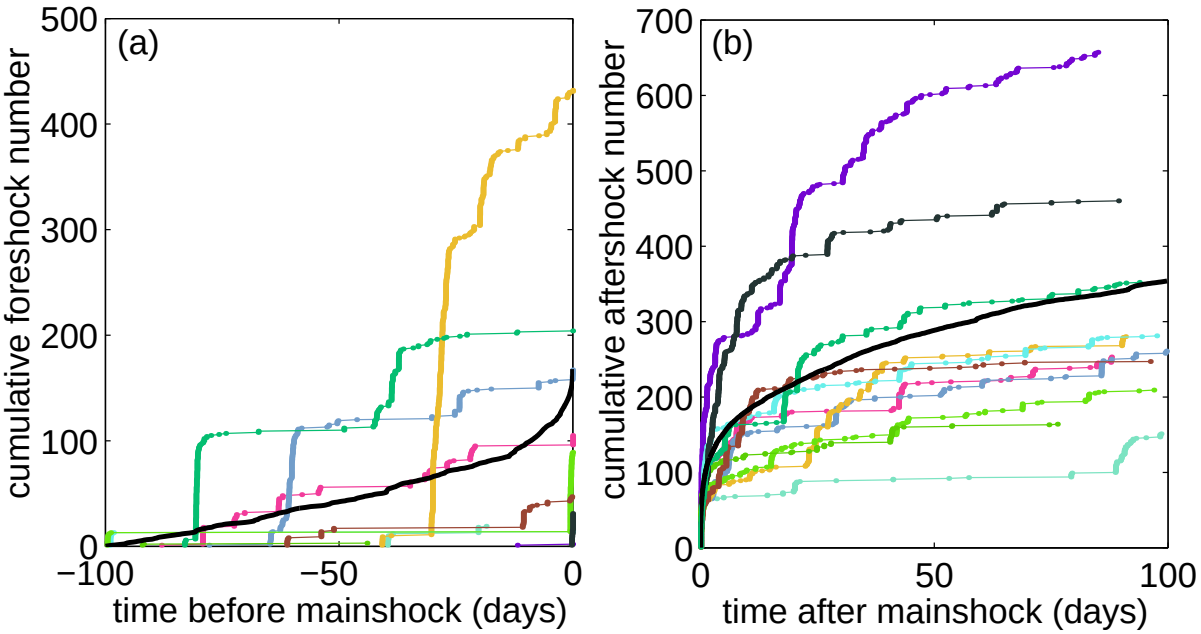

Figure 2. Typical foreshock (a) and aftershock (b) sequences generated by the ETAS model, for mainshocks of magnitude $M = 5.5$ occurring at time $t = 0$. We show 11 individual sequences in each panel. The solid black line represents the mean seismicity rate before and after a mainshock of magnitude $M = 5.5$, estimated by averaging over 250 sequences. The synthetic catalogs have been generated using the parameters $n = 1$, $\theta = 0.2$, and $a = 0.5\beta$, with a minimum magnitude threshold $m_0 = 2$. In contrast with the direct Omori law, which is clearly observed after any large mainshock, there are large fluctuations from one foreshock sequence to another one, and the inverse Omori law (with accelerating seismicity) is only observed when averaging over a large number of foreshock sequences.

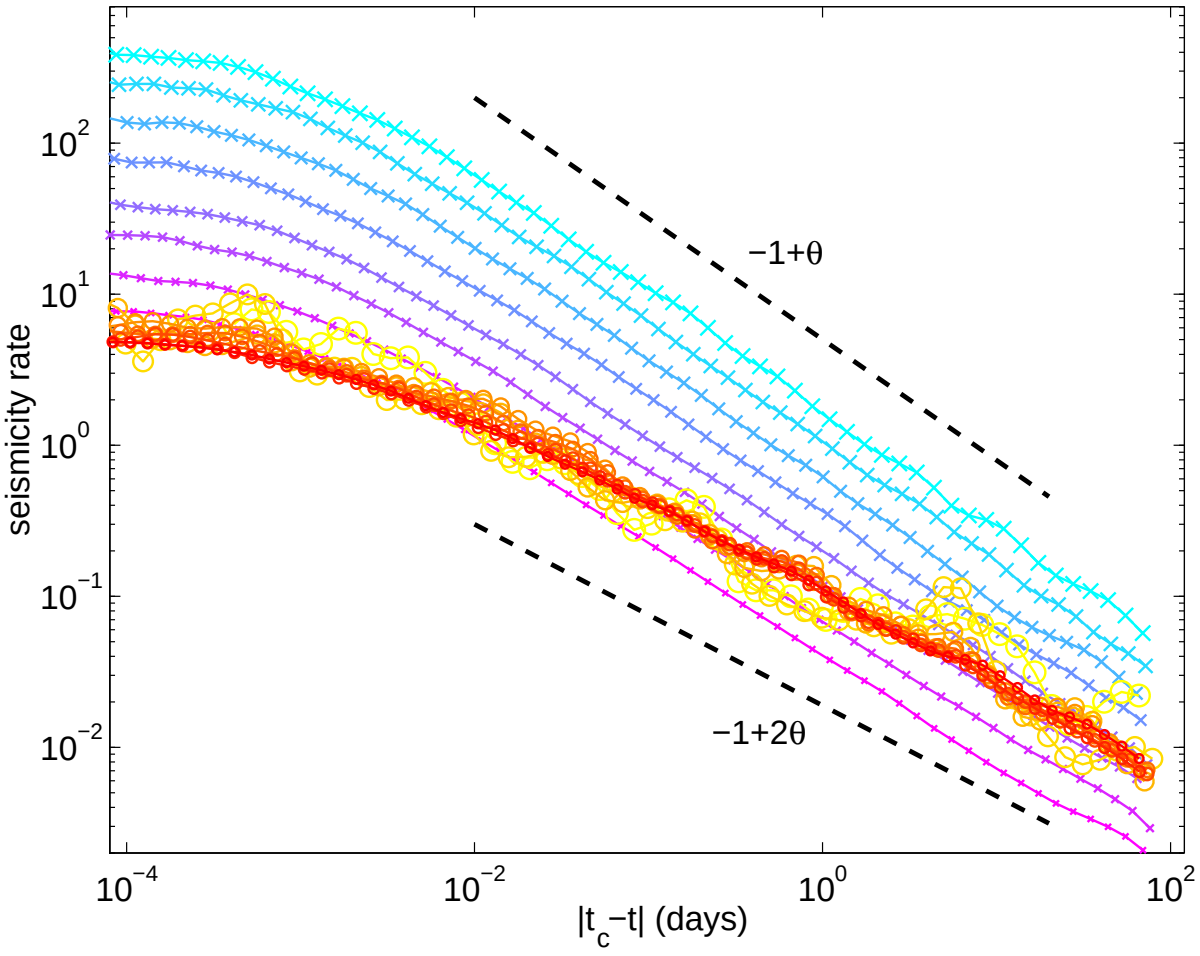

Figure 3. Direct and inverse Omori law for a numerical simulation with $a = 0.5\beta$ and $\theta = 0.2$ showing the two exponents $p = 1 - \theta$ for aftershocks and $p' = 1 - 2\theta$ for foreshocks of type II. The rate of aftershocks (crosses) and foreshocks (circles) per mainshock, averaged over a large number of sequences, is shown as a function of the time $|t_c - t|$ to the mainshock, for different values of the mainshock magnitude between 1.5 and 5, with a step of 0.5. The symbol size increases with the mainshock magnitude. The truncation of the seismicity rate for small times $|t_c - t| \simeq 0.001$ day is due to the characteristic time $c = 0.001$ day in the bare Omori propagator $\Psi(t)$, and is the same for foreshocks and aftershocks. The number of aftershocks increases with the mainshock energy as $N \simeq E^a$, whereas the number of foreshocks of type II in independent of the mainshock energy.

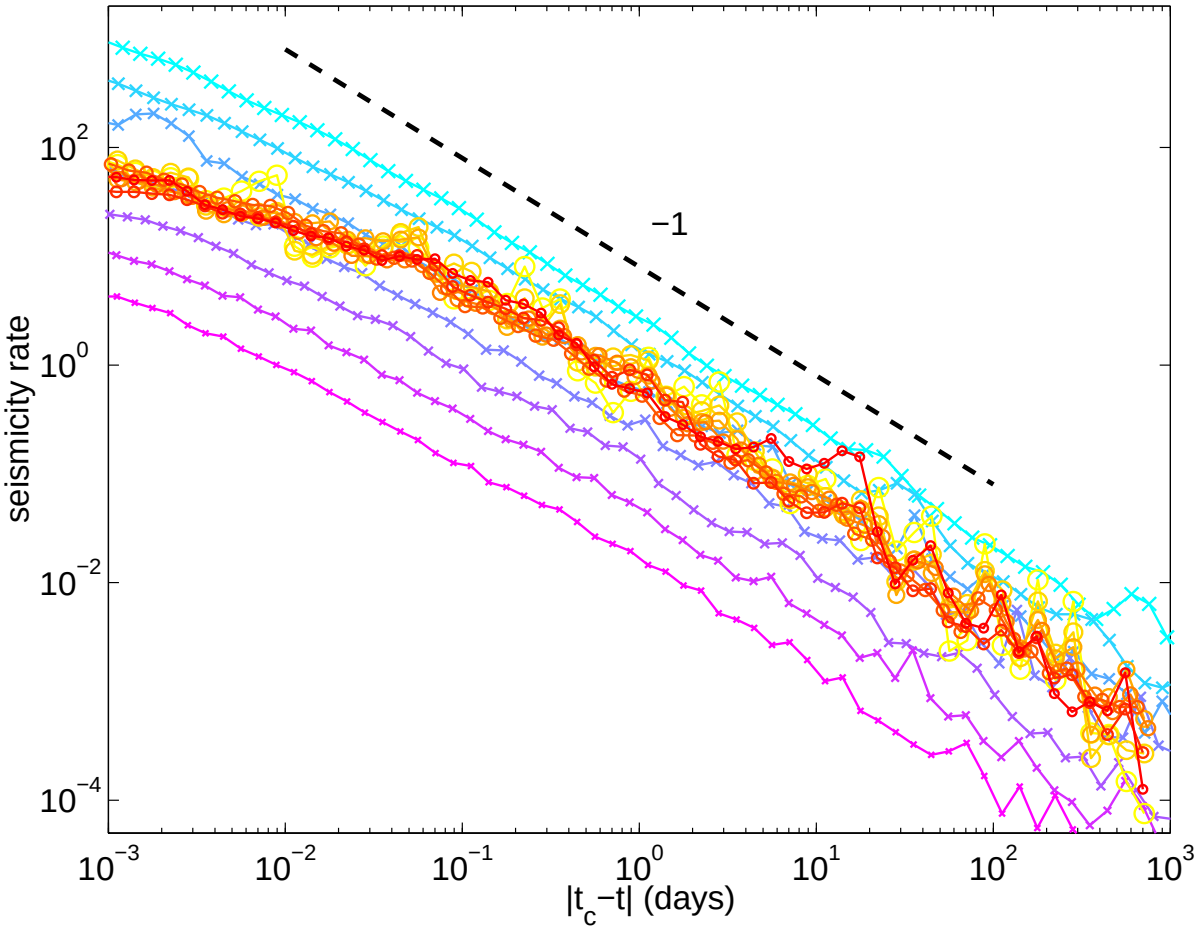

Figure 4. Same as Figure 3 for $a = 0.8\beta$, showing the larger relative ratio of foreshocks to aftershocks compared to the case $a = 0.5\beta$.

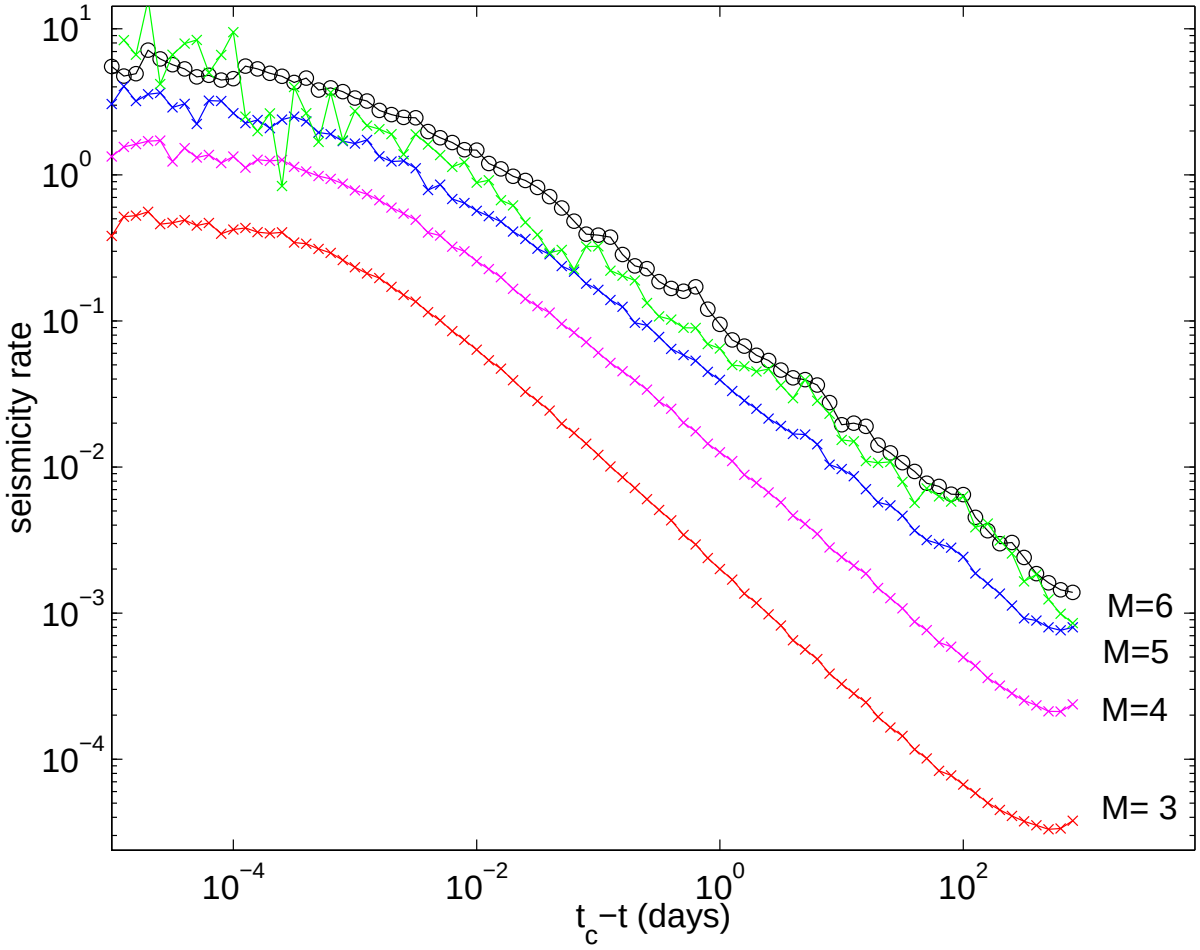

Figure 5. Foreshock seismicity rate per mainshock for foreshocks of type II (circles) and foreshocks of type I (crosses), for a numerical simulation with $n = 1$, $c = 0.001$ day, $\theta = 0.2$, $a = 0.5\beta$ and $m_0 = 2$. For foreshocks of type I, we have considered mainshock magnitudes M ranging from 3 to 6. We have rejected from the analysis of foreshocks of type I all mainshocks which have been preceded by a larger event in a time interval extending up to $t = 1000$ days preceding the mainshock. The rate of foreshocks of type II is independent on the mainshock magnitude M, while the rate of foreshocks of type I increases with M. For large mainshock magnitudes, the rate of foreshocks of type I is very close to that of foreshocks of type II. The conditioning that foreshocks of type I must be smaller than their mainshock induces an apparent increase of the Omori exponent p' as the mainshock magnitude decreases. It induces also an upward bending of the seismicity rate at times $t \approx 1000$ days, especially for the small magnitudes.

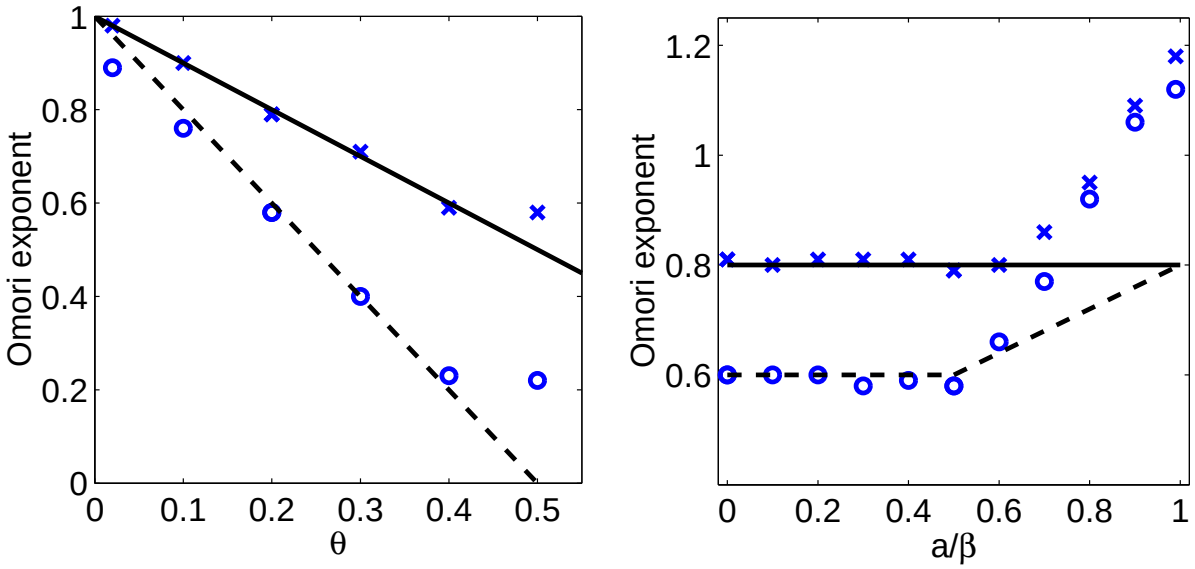

Figure 6. Exponents p' and p of the inverse and direct Omori laws obtained from numerical simulations of the ETAS model. The estimated values of p' (circles) for foreshocks and p (crosses) for aftershocks are shown as a function of θ in the case $\alpha = 0.5$ (a), and as a function of a/β in the case $\theta = 0.2$ (b). For a/β not too large, the values of p' for foreshocks are in good agreement with the predictions $p' = 1 - 2\theta$ for $a/\beta < 0.5$ (34) and $p' = 1 - \beta\ \theta/a$ for $a/\beta > 0.5$ (43). The theoretical values of p' are represented with dashed lines in each plot, and the theoretical prediction for p is shown as solid lines. For a/β not too large, the measured exponent for aftershocks is in good agreement with the prediction $p = 1 - \theta$ (16). For $a/\beta > 0.5$, both p and p'-values are larger than the predictions (16) and (43). For a/β close to 1, both p and p' are found close to the exponent $1 + \theta = 1.2$ of the bare propagator $\psi(t)$. See text for an explanation.

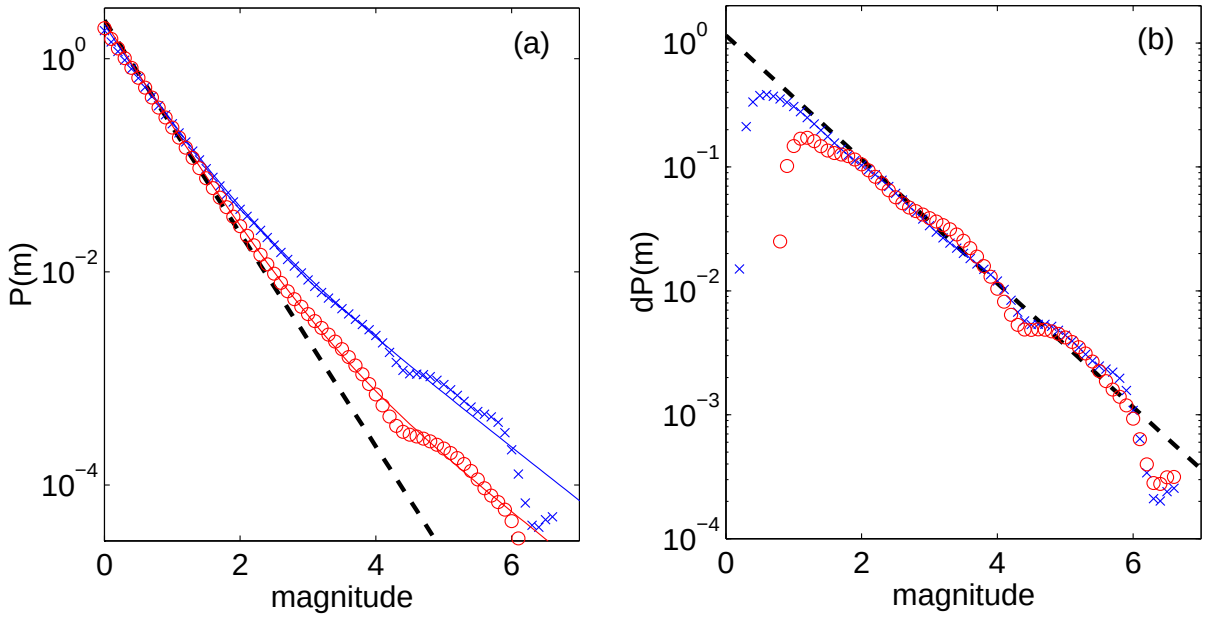

Figure 7. Magnitude distribution of foreshocks for two time periods: $t_c - t < 0.1$ days (crosses) and $1 < t_c - t < 10$ days (circles), for a numerical simulation of the ETAS model with parameters $\theta = 0.2$, $\beta = 2/3$, $c = 10^{-3}$ day, $m_0 = 2$ and $a = \beta/2 = 1/3$. The magnitude distribution $P(m)$ shown on the first plot (a) has been build by stacking many foreshock sequences of magnitudes $M > 4.5$ mainshocks. The observed magnitude distribution is in very good agreement with the prediction (51), shown as a solid line for each time period, that the magnitude distribution is the sum of the unconditional Gutenberg-Richter law with an exponent $b = 1.5\beta = 1$, shown as a dashed black line, and a deviatoric Gutenberg-Richter law $dP(m)$ with an exponent $b' = b - \alpha = 0.5$ with $\alpha = 1.5a = 0.5$. The amplitude of the perturbation increases if $t_c - t$ decreases as expected from (51). The observed deviatoric magnitude distribution $dP(m)$ is shown on plot (b) for the same time periods, and is in very good agreement with the prediction shown as a dashed black line. We must stress that the energy distribution is *no more* a pure power law close to the mainshock, but the sum of two power laws. The panel on the right exhibits the second power law which is created by the conditioning mechanism underlying the appearance of foreshocks. See text.

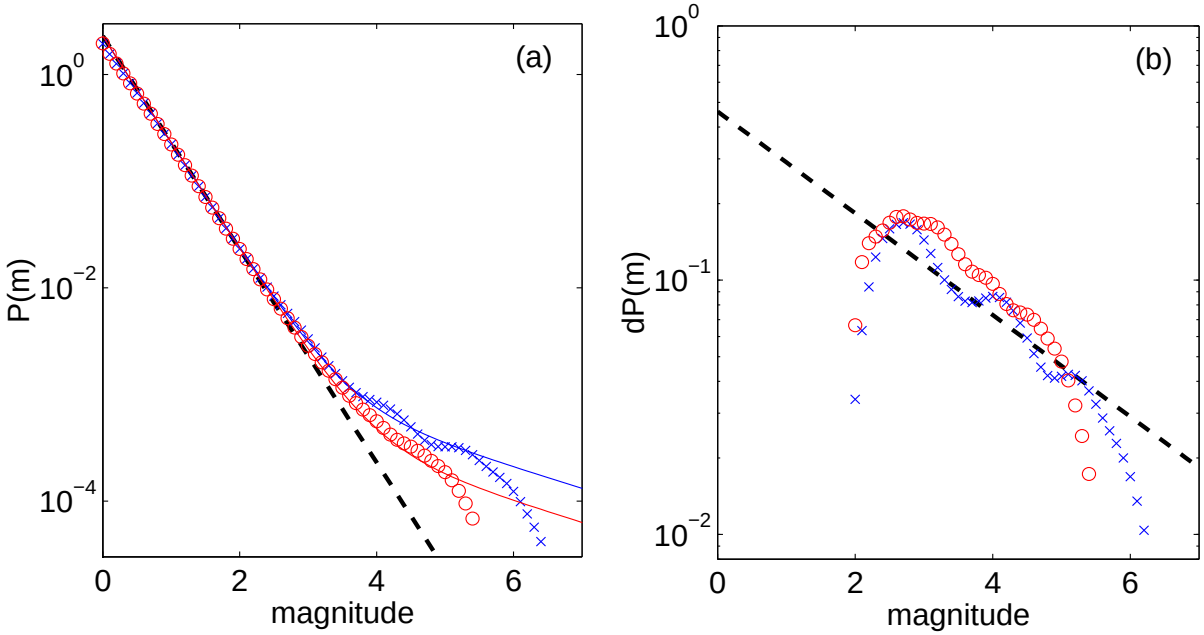

Figure 8. Same as Figure 7 but for $a = 0.8\beta$. In this case, the deviatoric Gutenberg-Richter contribution is observed only for the largest magnitudes, for which the statistics is the poorest, hence the relatively large fluctuations around the exact theoretical predictions.

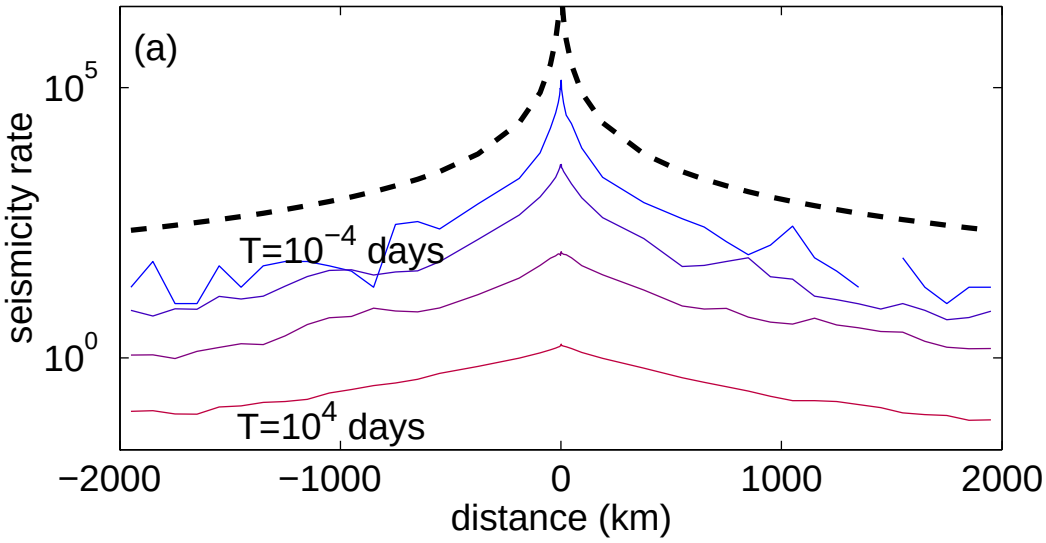
(a)
seismicity rate
10^5
10^0
T=10^{-4} days
T=10^4 days
−2000
−1000
0
1000
2000
distance (km)

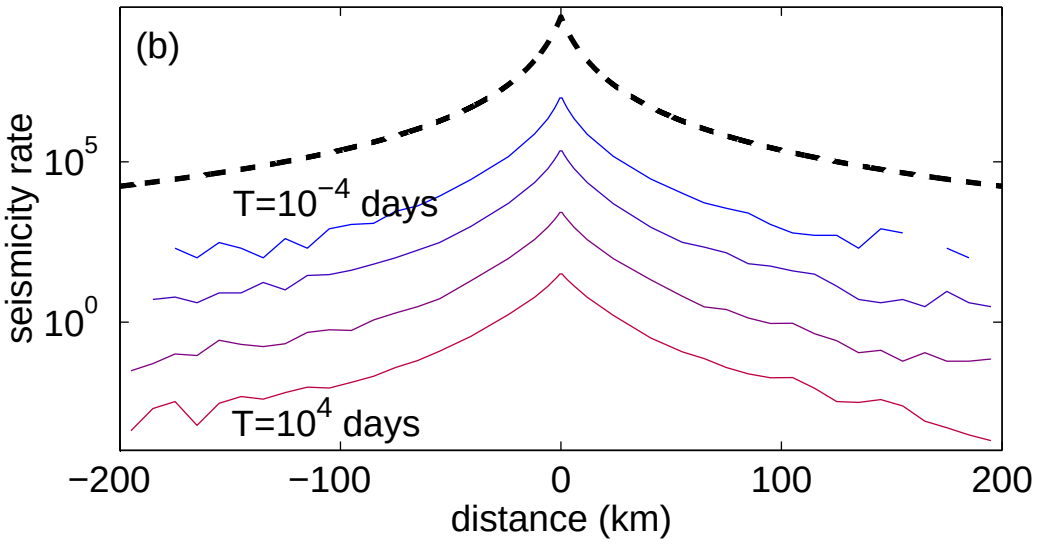
(b)
seismicity rate
10^5
10^0
T=10^{-4} days
T=10^4 days
−200
−100
0
100
200
distance (km)

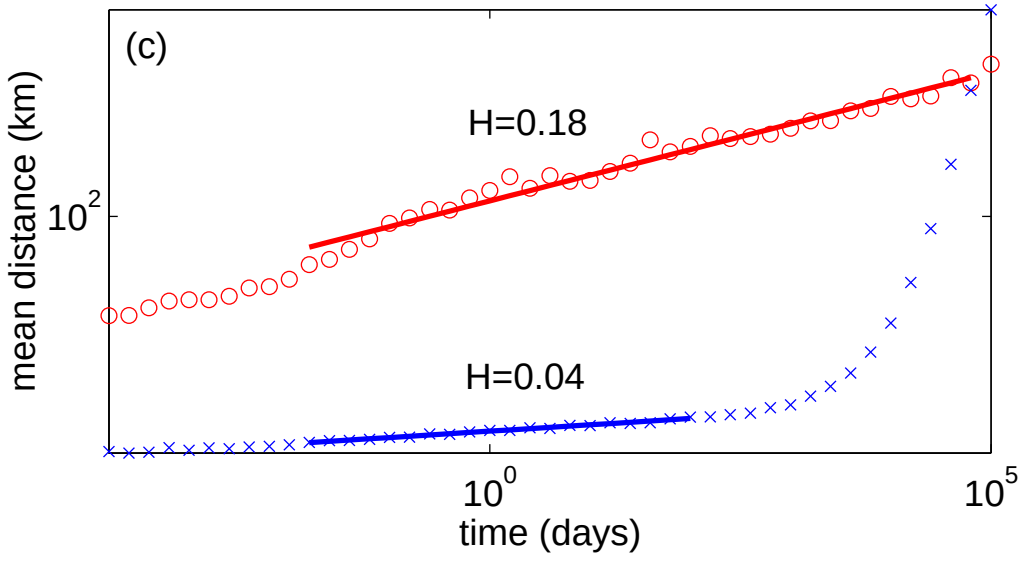
(c)
mean distance (km)
10^2
H=0.18
H=0.04
10^0
10^5
time (days)

Figure 9. Migration of foreshocks, for superposed foreshock sequences generated with the ETAS model for two choices of parameters, (a) $n = 1$, $\theta = 0.2$, $a = 0.5\beta$, $\mu = 1$, $d = 10$ km, $c = 0.001$ day, $m_0 = 2$ and (b) $n = 1$, $\theta = 0.02$, $a = 0.5\beta$, $\mu = 3$, $d = 1$ km, $c = 0.001$ day, $m_0 = 2$. The distribution of foreshock-mainshock distances is shown on panel (a) and (b) for the two simulations, for different time periods ranging between 10^{-4} to 10^4 days. The distribution of mainshock-aftershock distances given by (54) describing direct lineage is shown as a dashed line for reference. On panel (a), we see clearly a migration of the seismicity towards the mainshock, as expected by the significant diffusion exponent $H = 0.2$ predicted by (55). In contrast, the distribution of the foreshock-mainshock distances shown in panel (b) is independent of the time from the mainshock, as expected by the much smaller exponent diffusion $H = 0.01$ predicted by (55). The characteristic size of the foreshock cluster is shown as a function of the time to the mainshock on panel (c) for the two numerical simulations. Circles correspond to the simulation shown in panel (a) and crosses correspond to the simulation shown in panel (b). The solid line is a fit of the characteristic size of the foreshock cluster by $R \sim t^H$. For the simulation generated with $\theta = 0.2$ and $\mu = 1$ (circles), we obtain $H = 0.18 \pm 0.02$ in very good agreement with the prediction $H = \theta/\mu = 0.2$ (55). The simulation generated with $\theta = 0.02$ and $\mu = 3$ (crosses) has a much smaller exponent $H = 0.04 \pm 0.02$, in good agreement with the expected value $H = \theta/2 = 0.01$ (55). A faster apparent migration is observed at large times for this simulation, due to the transition from the uniform background distribution for large times preceding the mainshock to the clustered seismicity prior to the mainshock.

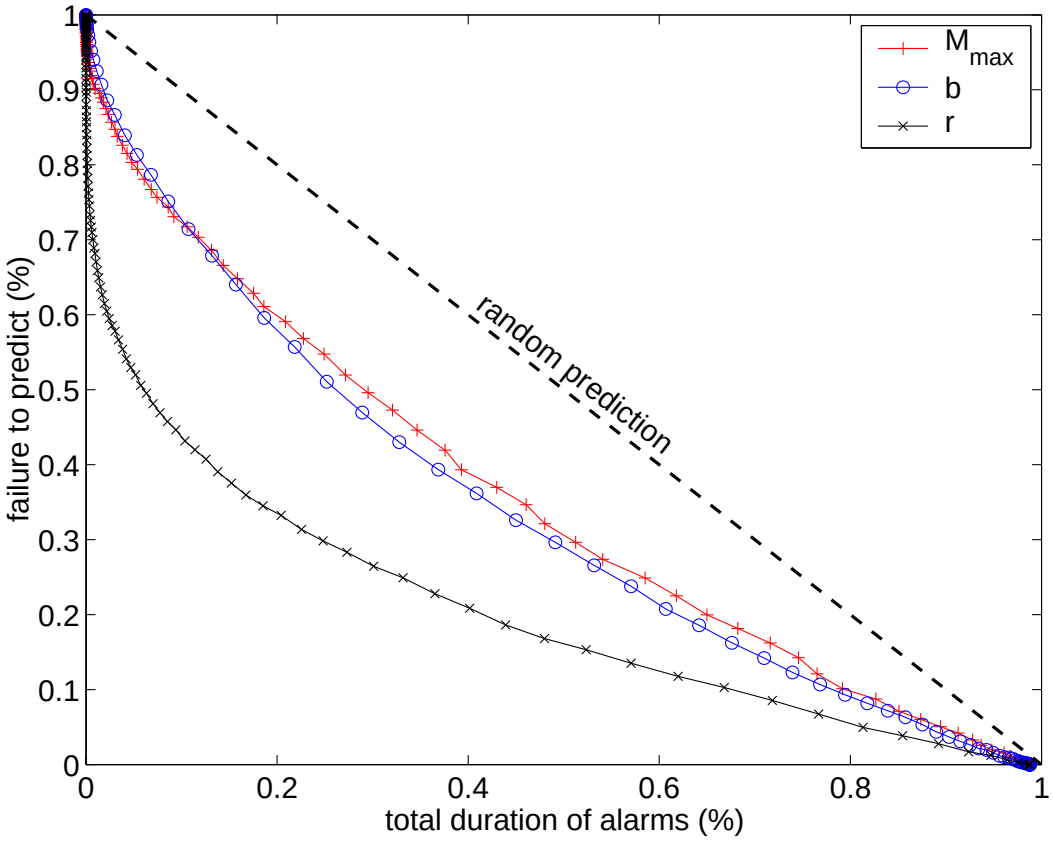

Figure 10. Results of prediction tests for synthetic catalogs generated with the parameters $a = 0.5\beta$, $n = 1$, $\beta = 2/3$, $\theta = 0.2$, $c = 0.001$ day and a constant source $\mu = 0.001$ shocks per day. The minimum magnitude is $m_0 = 3$ and the target events are $M \geq 6$ mainshocks. We have generated 500 synthetics catalogs of 10000 events each, leading to a total of 4735 $M \geq 6$ mainshocks. We use three functions measured in a sliding window of 100 events: (i) the maximum magnitude M_{max} of the 100 events in that window, (ii) the apparent Gutenberg-Richter exponent β measured on these 100 events by the standard Hill maximum likelihood estimator and (iii) the seismicity rate r defined as the inverse of the duration of the window. For each function, we declare an alarm when the function is either larger (for M_{max} and r) or smaller (for β) than a threshold. Once triggered, each alarm remains active as long as the function remains larger (for M_{max} and r) or smaller (for β) than the threshold. Scanning all possible thresholds constructs the continuous curves shown in the error diagram. The quality of the predictions is measured by plotting the ratio of failures to predict as a function of the total durations of the alarms normalized by the duration of the catalog. The results for these three functions are considerably better than those obtained for a random prediction, shown as a dashed line for reference. The best results are obtained using the seismicity rate. Predictions based on the Gutenberg-Richter β and on the maximum magnitude observed within the running window provide similar results.